

16th International Workshop Micromachined Ultrasonic Transducers

Event Programme
28th - 29th June 2017



MUT 2017 is Sponsored by



MUT 2017 gratefully acknowledges support provided by



Glasgow City Council



Glasgow Marketing Bureau

16th International Workshop on Micromachined ultrasonic transducers MUT 2017



Welcome

I welcome you all to the 2017 Micromachined Ultrasonic Transducers Workshop (MUT2017). It is a pleasure to host the meeting and to welcome a diverse array of scientists and engineers from industry and academia, united in the theme of design, manufacture, analysis and application of micromachined ultrasonic devices and transducers. The conference is a forum to exchange results, ideas and concepts whilst meeting old friends and forging new relationships.

Here's to a successful meeting and I do very much wish you pleasant and enjoyable stay in Glasgow.

Richard O'Leary

Scientific Scope of the Meeting

Concepts and fundamentals

Technologies

Processing, fabrication and materials

Electronics interfacing and packaging

Modelling: nonlinearities, FE simulation, cross-talk

Device Characterization

Applications

Scientific Committee

Abdullah Atalar, Bilkent University, Turkey

Giosuè Caliano, University Roma Tre, Italy

Levent Degertekin, Georgia Institute of Technology, Atlanta, USA

Jean-Francois Gelly, GE, France

B. T. Khuri-Yakub, Stanford University, USA

Mario Kupnik, DU Darmstadt, Germany

Paul Mural, EPFL, Switzerland

Arne Rønnekleiv, NTNU, Norway



Polytec is a global corporation with facilities in Europe, North America and Asia. With a reputation for innovative optical products, outstanding quality and world-class support, our success has enabled investment in the resources and flexibility to respond quickly to the ever-changing measurement needs of our customers.

Polytec's innovative measurement solutions allow our customers to maintain their own technical leadership across many fields. In markets from automotive, data storage and aerospace to biomedical, micro- and nano-technology, Polytec continues to lead and inspire confidence and trust from our customers. In addition, product distribution remains as a core competency of Polytec, through successfully representing manufacturers of innovative technologies.



Lyncée Tec SA is the leading company in the field of 4D optical microscopy. Its unique technology, based on digital holography (DHM®), provides simultaneously high acquisition rate and interferometric resolution.

It opens new quality control possibilities and novel research opportunities, enabling applications that were not possible before. Lyncée Tec offers complete characterisation solutions, from sample handling to data analysis, in the field of micro-production, MEMS, semiconductor, micro-optics, watch-making and cell imaging.



PZFlex is an FEA package specifically designed for simulating ultrasonic transduction and wave propagation. Its highly efficient time domain solvers allow problems to be solved orders of magnitude faster than general purpose packages, allowing larger, more realistic simulations to be tackled.

PZFlex has been used to simulate Micromachined Ultrasonic Transducers for over 15 years. With the capability for both piezoelectric & electrostatic calculations, users can create and analyse in 3D array structures to investigate Key Performance Metrics such as inter-element cross-talk, transmit-receive sensitivity, bandwidth and anything else captured during experimentation.

Through PZFlex, engineers can drastically reduce the requirement for physical fabrications and drive down development costs.



Windsor Scientific supplies and supports instruments for surface science, representing a number of independent, innovative manufacturers, including Lyncée Tec, in the UK and Ireland.

Our current range includes ambient AFMs and STMs, low temperature UHV SPMs, as well as instruments for 3D optical inspection such as stand-alone and mountable confocal/interferometry/focus variation microscopes and live 3D profilometers and MEMS characterisation tools based on Digital Holographic Microscopy. Now in our 28th year trading we continue to provide scientists and educators with innovative systems for R&D and education as well as quality control equipment for industry.

General Information

WiFi Access

WiFi access is provided throughout the conference venue and delegates have two options to connect to the network. Delegates affiliated to an academic or educational institution that participates in the Education Roaming Service can access WiFi via the SSID **eduroam** employing your usual authentication credentials.

Alternatively, WiFi can be accessed by selecting the SSID **WiFi Guest**

Once you have selected **WiFi Guest**, launch your preferred browser and select Go



You will then be asked to create or login to an existing **Cloud WiFi** account. If you have created a **Cloud WiFi** account at another establishment you may use these credentials to access this service, otherwise choose the Create Account option as shown below.

A screenshot of a web page for "University of Strathclyde Glasgow" and "WiFi Powered by The Cloud". The page has a dark blue header with a home icon and "Login / Registration". Below the header is a section titled "Account Sign In" with two input fields: "Email" and "Password". A "(Forgotten password?)" link is next to the password field. A dark blue "Continue" button is centered below the fields. Below the sign-in section is a "Don't have an account?" section with "Create Account" and "Products" links, each with a right-pointing arrow. At the bottom, there are links for "Terms", "Privacy & Cookies", and "About Us".

Enter all information requested and select Continue

You can use this service so long as you agree that The Cloud, its group companies and selected third parties may use your information to communicate with you for marketing purposes.

To register for The Cloud service you must accept our [Terms & Conditions](#) and [Privacy & Cookies notice](#)

Clicking on Continue means you accept our terms.

Continue

[Terms](#) [Privacy & Cookies](#) [About Us](#)

WLAN service provided by The Cloud Networks Ltd
© 2014 The Cloud Networks

2056498

You are now online with The Cloud

General Information

Civic Reception

The Civic reception hosted by The Rt Hon The Lord Provost of Glasgow at the Glasgow City Chambers at 19h00 Wednesday 28 June 2017. The reception will be followed by dinner served in the City Chambers.

Glasgow City Chambers is a short walk, approximately 5-6 minutes, from the conference venue. All delegates and guests are welcome.



Glasgow City Chambers

Social Event

At the conclusion of the technical programme on Thursday 29 June a private coach will transport delegates and guests to the Riverside Museum. Opened in May 2013 in a Zaha Hadid designed building, the Riverside Museum Collection covers the city's history as an industrial and maritime powerhouse, through the 20th Century to the Modern Day. City of Glasgow Tour guides will be on hand to assist delegates and guests in navigating the cultural a broad and eclectic range of artefacts.

The journey to and from the museum will encompass a tour of the architectural history of the City of Glasgow.



Riverside Museum and Tall Ship

08:30 Registration

09:15 Welcome

Session 1 - Fabrication I

Chair: Erik Vilain Thomsen, Technical University of Denmark

09:30 Investigation of the acoustic properties of porous silicon layers used as backing for CMUT
J. Lascaud, C. Compère, T. Defforge, A. Boulmé, D. Alquier, G. Gautier and D. Certon
Université François Rabelais de Tours, CNRS, CEA, INSA-CVL, GREMAN UMR7347, 16 Rue P. et
M. Curie, 37071 Tours, Cedex 2, France

09:50 High-frequency Ultrasound Arrays using Micromachined Single Crystal 1-3 Composites
Sibo Li, Huaiyu Wu and Xiaoning Jiang
North Carolina State University, Raleigh, NC, USA

10:10 Vented CMUT Design for Wide Bandwidth Airborne Applications
H. K. Oguz, B. Ma, C. Chang, K. Firouzi, and B. T. Khuri-Yakub
E. L. Ginzton Laboratory, Stanford University, Stanford, CA 94305

10:30 Coffee

Session 2 - Fabrication II

Chair: Abdullah Atalar, Bilkent University

11:00 Process optimisation of BCB-polymer for use in row-column addressed CMUTs
Martin Lind Ommen, Andreas Havreland, and Erik Vilain Thomsen
Department of Micro and Nanotechnology, Technical University of Denmark, Lyngby,
Denmark

11:20 Row-column addressed CMUT based on the polymer BCB
Andreas Spandet Havreland, Martin Lind Ommen, Chantal Silvestre, Mathias Engholm, and
Erik Vilain Thomsen
Department of Micro and Nanotechnology, Technical University of Denmark, Kgs. Lyngby,
Denmark

11:40 Pad printing as an enabling technology for capacitive transducer manufacture
James T. Andrews¹, Andrew Tweedie², Richard L. O'Leary¹
¹Dept. of Electronic and Electrical Engineering, University of Strathclyde, Glasgow, Scotland,
UK
²PZFlex, Glasgow, UK

12:00 "Pipe Organ" Air-coupled Broad Bandwidth Transducer
Botong Zhu¹, Benjamin Tiller¹, Alan J. Walker³, James F.C. Windmill¹, Anthony J. Mulholland²
¹Centre for Ultrasonic Engineering, University of Strathclyde Glasgow G1 1XW, UK
²Department of Mathematics and Statistics, University of Strathclyde Glasgow G1 1XH, UK
³School of Science and Sport, University of the West of Scotland Paisley PA1 2BE, UK

12:30 Lunch

Session 3 – Applications

Chair: Levent Degertekin, Georgia Institute of Technology

- 13:30 Combined colorimetric and gravimetric CMUT sensor for detection of phenylacetone
Mathias J.G. Mølgaard, Milan Laustsen, Ida L. Thygesen, Mogens H. Jakobsen & Erik V. Thomsen
DTU Nanotech, Technical University of Denmark, Kgs. Lyngby, Denmark,
- 13:50 Feasibility of interstitial MR-guided high intensity ultrasound heating with CMUTs: in-vivo study in pig brain
W. Apoutou N'Djin¹, Jérémy Vion¹, Loïc Daunizeau¹, Christopher Bawiec¹, Guillaume Bouchoux^{1,2}, Nicolas Sénégon³, Jean-Yves Chapelon¹, Alexandre Carpentier²
¹Inserm, U1032, LabTAU, Université Lyon 1, Lyon, F-69003, France
²CarThera Research Team, Brain and Spine Institute, Pitié Salpêtrière Hospital, Paris, France
³Vermon SA, Tours, 37038, France
- 14:10 Recent Advancements on the Development of CMUT Probes for 2D and 3D Medical Ultrasound Imaging
Alessandro Stuart Savoia, Barbara Mauti, Giosuè Caliano
Department of Engineering, Roma Tre University, Rome, Italy
- 14:30 Investigation of a planar 64-element CMUT truncated annular phased array for creating thermal lesions in biological tissue
C. Bawiec¹, W.A. N'Djin¹, G. Bouchoux¹, N. Sénégon², N. Guillen³, J.Y. Chapelon¹
¹ Inserm, U1032, LabTau, Lyon, F-69003, France; Université, Lyon 1, Lyon, F-69003, France
² Vermon, Tours, 37038, France
³ EDAP TMS, Vaulx-en-Velin, 69120, France
- 14:50 Coffee

Session 4 - Electronics Integration

Chair: Richard O'Leary, University of Strathclyde

- 15:30 Integrated Receiver Electronics for a CMUT Array
Y. Kansu, C. Bulbul, H. Köymen, A. Atalar
Electrical and Electronics Engineering Department, Bilkent University, Ankara, Turkey
- 15:50 Supply-Doubled Pulse-Shaping Pulser and Supply-Inverted Bipolar
Gwangrok Jung¹, Amirabbas Pirouz¹, Coskun Tekes², F. Levent Degertekin^{*1,2}, and Maysam Ghovanloo¹
¹School of Electrical and Computer Engineering, Georgia Institute of Technology, Atlanta, Georgia, USA
²School of Mechanical Engineering at the Georgia Institute of Technology, Atlanta, Georgia, USA
- 16:10 CMOS-Design of a Cascadable Front-End ASIC for CMUT Arrays
Sandro G. Koch, Andreas Weder, Marcus Pietzsch, Andreas Heinig, Marco Kircher, Mario Grafe, Nicolas Lange, Jörg Amelung
Fraunhofer Institute for Photonic Microsystems (IPMS), Dresden, Germany,
- 16:30 Sponsor presentations
- 17:00 End of first day presentations
- 19:00 Civic reception and Dinner, Glasgow City Chambers

Session 5 – Simulation

Chair: Nicola Lamberti, Università di Salerno

- 09:15 Simulating CMUT Arrays Using Time Domain FEA
Mathias Engholm¹, Andrew Tweedie², Søren Elmin Diederichsen¹, Gerald Harvey³, Jørgen Arendt Jensen⁴, and Erik Vilain Thomsen¹
¹Department of Micro and Nanotechnology, Technical University of Denmark, Kgs. Lyngby, Denmark
²PZFlex, Glasgow, United Kingdom
³PZFlex, Cupertino, USA
⁴Center for Fast Ultrasound Imaging, Technical University of Denmark, Kgs. Lyngby, Denmark
- 09:35 A hybrid boundary element model for the simulation of large PMUT arrays in immersion
Bernard Shieh, Karim G. Sabra, F. Levent Degertekin
G.W. Woodruff School of Mechanical Engineering, Georgia Institute of Technology, Atlanta, GA USA,
- 09:55 Frequency-Tunability of a Collapse-Mode CMUT: from modelling to pre-clinical imaging
Martin Pekař^{1,2}, Nenad Mihajlović¹, Alexander F. Kolen¹, Harm Belt¹, Jeannet van Rens¹, Frank Budzelaar¹, Bas Jacobs¹, Frank van Heesch¹, Wendy U. Dittmer¹, Debbie Rem-Bronneberg¹, Stephan H. M. van Nispen³, Rob H. B. Fey³, Sergei Shulepov¹, Henk Nijmeijer³, Imo E. Hoefler⁴, Tamas Szili-Török², Hendrik J. Vos^{2,5}, Johan G. Bosch², Gijs van Soest², Nico de Jong^{2,5}, Antonius F. W. van der Steen^{2,5}
¹Philips Research, Eindhoven, the Netherlands
²Erasmus MC, Rotterdam, the Netherlands
³Department of Mechanical Engineering, Eindhoven University of Technology, the Netherlands
⁴Faculty of Veterinary Medicine, Utrecht University, the Netherlands
⁵Dept. of Imaging Physics, Delft University of Technology, Delft, the Netherlands
- 10:15 The Effect of Insulator Charging on CMUT Performance
Hayrettin Köymen¹, Abdullah Atalar¹, Saadettin Güler², İtir Köymen¹, A.Sinan Taşdelen², and Aslı Ünlügedik²
¹Electrical and Electronics Engineering Department, Bilkent University, Ankara, Turkey
²Bilkent University Acoustics and Underwater Technologies Research Center (BASTA), Bilkent University, Ankara, Turkey
- 10:35 Multiphysics Model and Experimental Validation of an Air-Coupled PMUT at 100 kHz
G. Massimino¹, L. D'Alessandro¹, F. Procopio², R. Ardito¹, M. Ferrera², A. Corigliano¹
¹Department of Civil and Environmental Engineering, Politecnico di Milano, Piazza Leonardo da Vinci 32, 20133 Milan, Italy
²Analog, MEMS & Sensors Group, ST Microelectronics, Via Olivetti 2, 20100 Agrate Brianza, Italy
- 10:55 Coffee

Session 6 – Characterisation

Chair: Giosue Caliano, University of Roma Tre

- 11:30 Characterization infrastructure for the CMUT platform
Chris van Heesch, Peter Dirksen & Marco de Wild
Philips Research, Eindhoven, The Netherlands
- 11:50 Output Pressure and Pulse-Echo Characteristics of CMUTs as Function of Plate Thickness
Søren Elmin Diederichsen, Jesper Mark Fly Hansen, Mathias Engholm, Jørgen Arendt Jensen,
& Erik Vilain Thomsen
Technical University of Denmark, 2800 Kgs. Lyngby, Denmark
- 12:10 Analysis and representation of DHM® data for MUT and SAW analysis
Yves Emery, Jérôme Parent, Eduardo Solanas & Etienne Cuche
Lyncée Tec SA, Lausanne, Switzerland
- 12:30 Lunch
- 13:45 MUT2017 Best Paper
- 14:00 MUT 2018
- 14:15 Discussion and Closing Remarks
- 14:45 Departure for Tour
- 18:00 Return to TIC Building

Investigation of the acoustic properties of porous silicon layers used as backing for CMUT

J. Lascaud, C. Compère, T. Defforge, A. Boulmé, D. Alquier, G. Gautier and D. Certon

Université François Rabelais de Tours, CNRS, CEA, INSA-CVL, GREMAN UMR7347, 16 Rue P. et M. Curie, 37071 Tours, Cedex 2, France

julie.lascaud@univ-tours.fr

Introduction

An acoustic backing is required on CMUT-based linear arrays to avoid artifacts in ultrasonic images due to the Lamb wave propagation in the substrate [1]. A millimeter-thick-backing film could be stuck on the rear side of the substrate but it prevents 3D packaging and increases device dimensions. The present study proposes the use porous silicon (PS) to attenuate these waves. Previous works on PS ultrasonic applications [2] were mainly focused in the GHz frequency range with water-filled pores. Acoustic characterizations reported in these papers showed a lower acoustic impedance and velocity with increasing porosity. However, no clear evidence was reported on the ultrasonic attenuation in PS. The first aim of this work was to study the influence of the air-filled PS layers on the thickness mode resonance (in the MHz frequency range). Therefore, the acoustic properties of Si wafer/PS bilayer, without CMUT, were investigated by means of a contact measurement. Secondly, PS was etched on the rear side of a CMUT wafer and its impact on transducer pulse-echo response was evaluated.

Experimental and results

PS layers were obtained by electrochemical etching of 510 μm -thick p+-type Si wafers, (100)-oriented. Branched-pores with size ranging from 6 nm to 10 nm are usually formed with this kind of highly-doped substrate [3]. Electrolyte was composed of 30 wt% hydrofluoric acid. The current density was fixed to 50 mA/cm² and duration was adjusted to get various PS thickness, layers characteristics are given in Fig. 1. A batch of CMUT wafers was fabricated onto the same highly-doped Si substrate by using a high temperature surface micromachining process. LPCVD polycrystalline silicon was used to form the bottom electrode. PECVD PhosphoSilicate glass was used as sacrificial layer to form a 200 nm gap cavity. The 450 nm-thick membranes of silicon nitride were deposited by LPCVD at 800 °C. Cells were covered by a patterned PVD aluminium. Eventually, the wafer rear side was grinded at the end of CMUT manufacturing to clean the Si surface from all the process contaminations. PS layer was etched in the same conditions that PS3 sample. Contact measurements were implemented to characterize the thickness mode resonance of the Si wafer/PS bilayer. A single element transducer was used with central frequency close to the thickness mode, i.e. 8.5 MHz. The input acoustic admittance of the Si/PS bilayer under test was extracted from the electrical impedance measurement of the ultrasonic transducer (UST). The UST was modelled as a two-port electrical network. The transfer matrix was determined from 3 measures of the UST electrical impedance, successively immersed in air, water and isopropyl alcohol.

Wafer level pulse-echoes tests were carried to measure electroacoustic response of CMUT circular-shaped elements of 2 mm-diameter, made with $20 \times 20 \mu\text{m}^2$ square membranes. Measurements were done in oil with microprobes and a standard high-frequency electronic pulser. Specific protection was placed around the transducer to maintain the rear face in contact with air and avoid oil infiltration in the porous layer. The bias voltage was fixed to 45 V and a 6 V negative pulse was added through a bias-tee.

The acoustic admittances of the PS samples are presented in Fig. 1. A particular attention is paid to the resonance peak of the thickness mode. Contrasts between Si and Si/PS bilayers peaks are observed for all the samples. The admittance peak shifts to higher frequencies with the increase in the PS thickness. Amplitude and quality factor of the resonance peaks clearly decrease with the increasing layer thickness. This behavior is in good agreement with the observations in [2]. The FFT of the pulse-echo responses of the CMUT circular-shaped elements with and without PS backing are shown in Fig. 2. A cutoff imputed to thickness mode resonance is observed on the spectrum of the element integrated on the Si. The notch amplitude varies from -35 dB, without backing, to -20 dB with PS backing. As for impedance measurement, substrate ringing frequency is increased of 0.3 MHz.

Conclusion

The acoustic properties of PS layers were investigated in order to use it as backing for CMUT. The influence of PS on the pulse-echo response of circular-shaped CMUT elements was estimated. Frequency responses of both transducers with and without backing show that PS substantially reduces the cutoff due to thickness mode resonance. Further measurements along elements of an array are currently being performed to quantify Lamb wave attenuation efficiency.

Acknowledgment

This work has been funded by the "Région Centre" in the frame of the SIPeMUT research project (2013-00083160). The authors would like to thank the Conseil Departemental d'Indre et Loire for their financial supports.

References

- [1] Oralkan, *et al.*, Ultrasonics, IEEE Transactions on Ferroelectrics, and Frequency Control, 49 (2002), 1596-1610
- [2] Aliev, G. N., *et al.*, Journal of Applied Physics, 110 (2011), 043534
- [3] Capelle, M., *et al.*, IEEE Transactions on Electron Devices, 62(2015), 4169-417

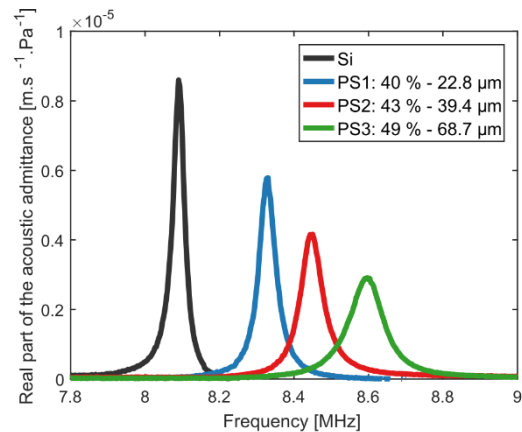


Fig. 1. Real part of the acoustic admittance of the 3 PS layers of various thicknesses etched at constant current density: PS1: 22.8 μm -thick and 40% of porosity (\rightarrow); PS2: 39.4 μm -thick and 43% of porosity (\rightarrow); PS3: 68.7 μm -thick and 49% of porosity (\rightarrow) compared to a 510 μm -thick Si (\rightarrow).

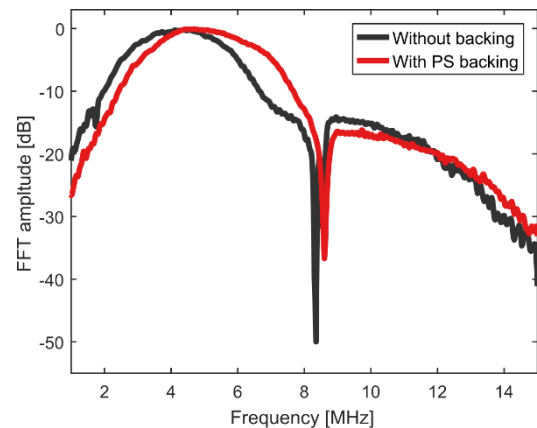


Fig. 2. FFT of the pulse-echo responses of the CMUT circular-shaped elements integrated on substrate without backing (\rightarrow) on substrate with PS backing (\rightarrow).

High-frequency Ultrasound Arrays using Micromachined Single Crystal 1-3 Composites

Sibo Li, Huaiyu Wu and Xiaoning Jiang

North Carolina State University, Raleigh, NC, USA

xjiang5@ncsu.edu

High frequency ultrasound transducers (> 20 MHz) are of increasing demand in recent years for medical imaging, acoustic microscopy, and biological particle manipulations. The performances of piezoelectric transducers greatly rely on the properties of the piezoelectric materials and transduction structures, including piezoelectric coefficient (d), electromechanical coupling coefficient (k), dielectric permittivity (ϵ) and acoustic impedance (Z). Piezo-composite structures are preferred because of their relatively high electromechanical coupling coefficient and low acoustic impedance. A number of piezo-composite techniques have been developed, namely “dice-and-fill”, “tape-casting”, “stack-and-bond”, “interdigital-phase-bonding”, “laser micromachining” and “micro-molding”. More recently, the piezo-composite micromachined ultrasound transducers (PC-MUT) technique was developed to fabricate high-performance, high-frequency piezo-composite ultrasound transducers [1]. In this paper, high frequency (> 30 MHz) piezoelectric 1-3 composite transducer arrays are demonstrated for ultrasound imaging.

The photolithography and deep-dry-ion-etching (DRIE) of PMN-PT single crystal were adopted for high frequency 1-3 composite fabrication. Those micromachining techniques have several advantages compared with conventional fabrication approaches, including submicron machining precision, batch fabrication, a low mechanical stress environment for fragile and fine structures, and the possibility for integrated array design. For high-frequency composite fabrication, PMN-PT single crystal wafers were coated with Ni as an electroplating seed layer on the polished side. Ni coated PMN-PT wafers were next coated with photoresist using a spin coater. UV exposure based photolithography was conducted to form a periodical array pattern. A through-wafer Ni electroplating process was then used to grow the Ni posts out of the photoresist template as the hard mask for further etching step. After plating, the photoresist was stripped off. The PMN-PT wafer with Ni etching mask was then put into the dry etching chamber for deep reactive ion etching. Epoxy was filled into the kerfs of etched PMN-PT single crystal post as epoxy filler. The wafer was lapped on one side to expose the PMN-PT posts and then flipped over for the second side

lapping until the final thickness was achieved. Both sides of the resulting 1-3 single crystal/epoxy composites were then sputtered with Cr and Au.

The feature size of single crystal pillars was about 15 μm in width. The kerf between pillars was less than 5 μm . 50-element 40-MHz linear array transducers with the pitch of 100 μm were fabricated and characterized using the micromachined 1-3 composites. Wire phantom imaging was conducted for imaging resolution evaluation. The pulse-echo tests showed that the center frequency is 39 ± 2 MHz and -6 -dB

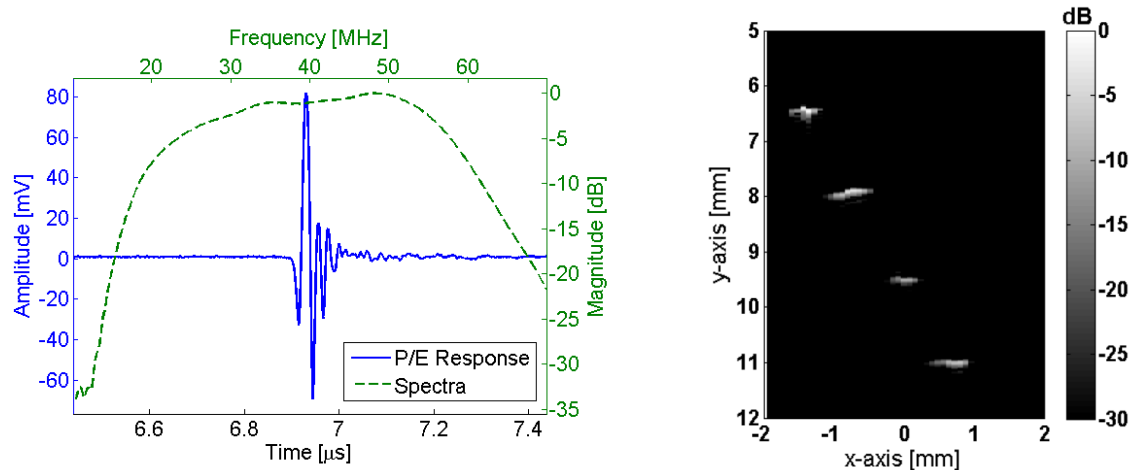


Fig. 1. Pulse-echo response from a representative element array (left), and an image of steel wires reconstructed by synthetic aperture method, with the dynamic range of 30 dB (right).

fractional bandwidth is $75\pm 6\%$ (Fig. 1). The insertion loss is -26 dB, and crosstalk between adjacent elements is about -25 dB. Imaging testing with phantom wires (diameter of 50 μm) was conducted with a dynamic range of 30 dB. The penetration depth of 12 mm was processed using the synthetic aperture method. The -6 dB beamwidth was estimated to be 70 μm in the axial direction at a distance of 8 mm away from the probe. The results suggest that the 40 MHz micromachined 1-3 composite linear arrays are promising for medical imaging applications.

References

- [1] J. Yuan, X. Jiang, K. Snook, P. Rehrig, T. Shrout, W. S. Hackenberger, *et al.*, "5I-1 Microfabrication of piezoelectric composite ultrasound transducers (PC-MUT)," in *Ultrasonics Symposium, 2006. IEEE*, 2006, pp. 922-925.

Vented CMUT Design for Wide Bandwidth Airborne Applications

H. K. Oguz, B. Ma, C. Chang, K. Firouzi, and B. T. Khuri-Yakub
E. L. Ginzton Laboratory
Stanford University
Stanford, CA 94305

In airborne ultrasound applications, there is a need to develop wide bandwidth transducers for improved axial resolution. The smaller ring-down times due to a wider bandwidth also enable faster measurement rates. As for most MEMS devices, CMUTs with narrow air gaps experience significant air damping and stiffening due to the squeeze film action. By properly selecting the size, number, and location of the venting holes that pressurize the cavity, the squeeze film effect can be controlled to optimize the dynamic behavior of the transducer.

We have demonstrated CMUT designs with cavities vented either through the plate or through the substrate for use in ultrasonic flowmeter applications. While having holes through the plate makes it easier to fabricate and package the device, having holes through the substrate allow us to separate the air inside the cavity from the potentially harsh environment. We have developed finite element models using COMSOL Multiphysics. The model is subdivided into multiple domains, where the corresponding physics are solved and coupled through the respective boundaries.

Using this model, we designed CMUTs with varying sensitivity and bandwidth. COMSOL uses Navier-Stokes equations to model the fluid losses accurately. Thus, we may separately calculate the viscous and thermal losses inside the air cavity and holes, in addition to the delivered electrical power and radiated acoustic power. Thus, the insertion loss of the vented CMUT can be obtained at different configurations. We will present results of a 1 MHz design with excellent depth resolution for gas flow metering applications.

Process optimisation of BCB-polymer for use in row-column addressed CMUTs

*Martin Lind Ommen*¹, *Andreas Havreland*¹, and *Erik Vilain Thomsen*¹

¹Department of Micro and Nanotechnology, Technical University of Denmark, Kgs. Lyngby, Denmark

marlio@nanotech.dtu.dk

By addressing 2-D transducer arrays in a row-column (RC) scheme, instead of a matrix addressing scheme, the number of connections can be reduced, for the same number of rows and columns of the array. This can decrease the production costs significantly. However, it has been seen that as the device footprint increases, the fabrication of RC CMUTs becomes challenging. One of the reasons is due to the conventional bonding methods of either direct- or anodic bonding of the plate to the material defining the CMUT cavities, which is often SiO₂. These bonding methods are sensitive to particles, and even single particles can ruin full arrays. The particles introduce stresses, which can be increased further by the high temperature processes.

Benzocyclobutene (BCB) is an alternative to SiO₂, which can not only function as the cavity defining material, but also decrease the particle sensitivity of the bonding process, as it can be used for adhesive bonding. In addition, the maximum processing temperature will be limited by the curing temperature of the BCB, which is done below the glass transition temperature of 350 °C. But implementing BCB for large footprint RC CMUTs will require good wafer uniformity of film parameters, such as film thickness, and electrical breakdown field, and will at this point require optimisation of the BCB processing.

The documentation provided by the manufacturer, DOW, suggests a potential breakdown field of 0.53 V/nm. This is low compared to SiO₂ which has a breakdown field of ~1 V/nm. Furthermore, the actual breakdown field of BCB is highly dependent on the curing of the BCB-polymer. The curing scheme for BCB suggested by DOW is a two-step temperature treatment, which can be represented as in Figure 1. DOW has specified standard curing temperatures and times for both plateaus. However, using the suggested parameters consistently yields a much lower breakdown voltage than the ideal 0.53 V/nm, with the largest documented operational field being 0.38 V/nm [Li et al., 2016].

Fourier transform infra-red spectroscopy (FTIR) has previously been used to determine the curing level of the BCB [Beechinor et al., 1997]. A FTIR spectrum of a BCB film can be seen in Figure 2. As the level of curing increases, the absorption will increase at 1500 cm⁻¹, and will decrease at 1475 cm⁻¹ [Beechinor et al., 1997]. This change can then be used to quantify the level of curing.

We will present an optimised curing method for BCB, based on, and optimised by, statistical modelling, which approaches the ideal breakdown field of 0.53 V/nm. In addition, the systematic variation in the FTIR spectra with the increased electrical properties will be reported. As Si is transparent in the infra-red part of the light spectrum, using FTIR will allow characterising the BCB, even for finished, wafer bonded, devices.

References

- [Beechinor et al., 1997] Beechinor, J. T., McGlynn, E., O'Reilly, M., and Crean, G. M. (1997). Optical characterization of thin film benzocyclobutene (BCB) based polymers. *Microelectronic Engineering*, 33(1-4).
- [Li et al., 2016] Li, Z., Wong, L. L. P., Chen, A. I. H., Na, S., Sun, J., and Yeow, J. T. W. (2016). Fabrication of capacitive micromachined ultrasonic transducers based on adhesive wafer bonding technique. *Journal of Micromechanics and Microengineering*, 26(11):115019.

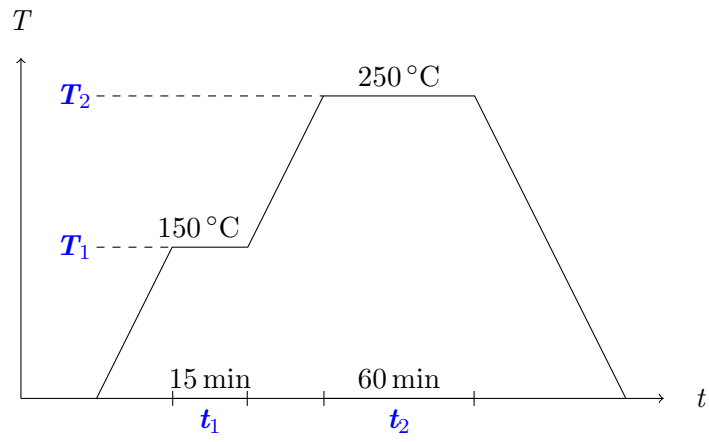


Figure 1: Two-step curing scheme suggested by DOW, with two different curing temperatures and times. The noted processing parameters are those suggested by DOW.

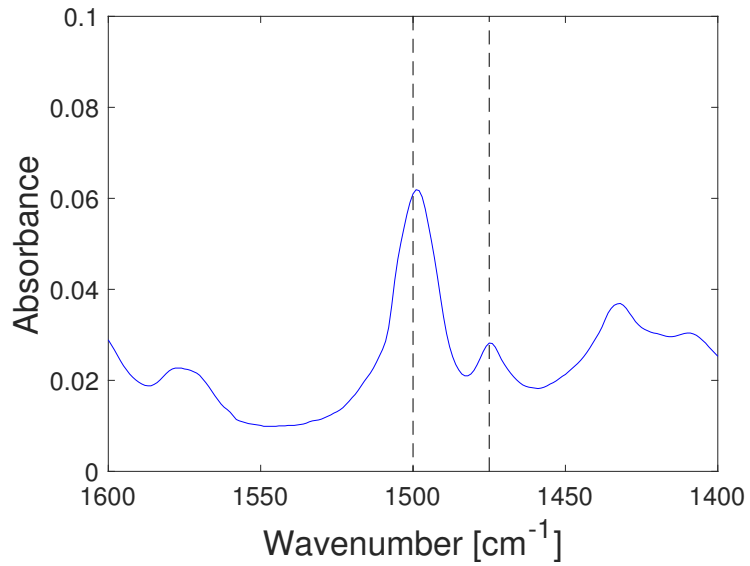


Figure 2: Measured FTIR spectra of BCB with dashed lines showing the peaks at 1475 cm^{-1} and 1500 cm^{-1} .

Row-column addressed CMUT based on the polymer BCB

Andreas Spandet Havreland¹, Martin Lind Ommen¹, Chantal Silvestre¹, Mathias Engholm¹, and Erik Vilain Thomsen¹

¹Department of Micro and Nanotechnology, Technical University of Denmark, Kgs. Lyngby, Denmark

ahav@nanotech.dtu.dk

The number of transmit and receive channels needed to perform real-time 3-D ultrasonic imaging can be greatly reduced if row-column (RC) addressed 2-D transducer arrays are used. However, fabricating RC CMUTs have shown to be challenging. The difficulties are typically stress issues related to the high temperature processes and dielectric charging, overall resulting in low yield and/or a time dependent performance. To overcome these problems, a polymer adhesive bonding using Bisbenzocyclobutene (BCB) can be applied. Previous work [1,2] has shown promising results for a single element. This contribution presents a realization of BCB RC CMUTs utilizing BCB-to-Silicon bonding.

A 62+62 RC 3.0 MHz CMUT is fabricated in a 3 mask process. A fabrication sketch and a microscope image of the presented CMUT is shown in Figure 1. A quartz wafer is used as a bottom substrate to decrease the electric cross talk between the CMUT cells. The fabrication consists of the following steps: (Step 1) Deposit and pattern metal on top of a quartz wafer. (Step 2) Spin-coat BCB on top and then pattern in a UV-lithography step. (Step 3) Bond a SOI wafer to the patterned BCB and etch away the handle layer and the buried oxide (BOX) in respectively a KOH and BHF etch. (Step 4) Finally, deposit a metal on top and open up to the bottom electrode in a dry etch process. The maximum temperature during the fabrication is the curing temperature of BCB at 250 °C. Hence, the process contains no high temperature process steps, thus lower thermal stress is expected. The presented design has a patterned bottom electrode surrounded by BCB (see Figure 1). CMUTs designed this way has minimized the electric field inside the BCB. Finally, due to the absence of dielectric thin films inside the cavities, charging phenomenons are not expected in this type of CMUT.

The presented BCB CMUTs have been electrically characterized by impedance and Capacitance versus Voltage (CV) measurements, shown in Figure 2. The impedance measurements show the expected behaviour of a CMUT, where a resonant peak is observed at 6 MHz. At resonance the phase angle goes from -90° to -20°. In the future the phase shift has to be improved.

Hysteresis in a CV curve indicates mobile charges, and the capacitance will depend on the voltage sweep direction. Potentially the CV curves can have an offset up to several volts depending on the sweep direction. The red data corresponds to a sweep going from -100V to 100V where the blue data is the opposite direction. No hysteresis is observed indicating the absence of mobile charges. The CV curve is expected to have a parabolic profile for $\frac{V}{V_{\text{pull-in}}} \ll 1$, and the data can thus be fitted to the function:

$$C(V) = C_0 \left[1 + k (V - V_{\text{offset}})^2 \right] \quad (1)$$

Where C_0 is the minimum capacitance, k is a curvature parameter and V_{offset} is the voltage offset. V_{offset} for the BCB data is identical within the estimation uncertainties. In conclusion the combination of simple and low temperature fabrication with no charging effects makes BCB a good candidate for solving the issues related to fabrication of RC CMUTs.

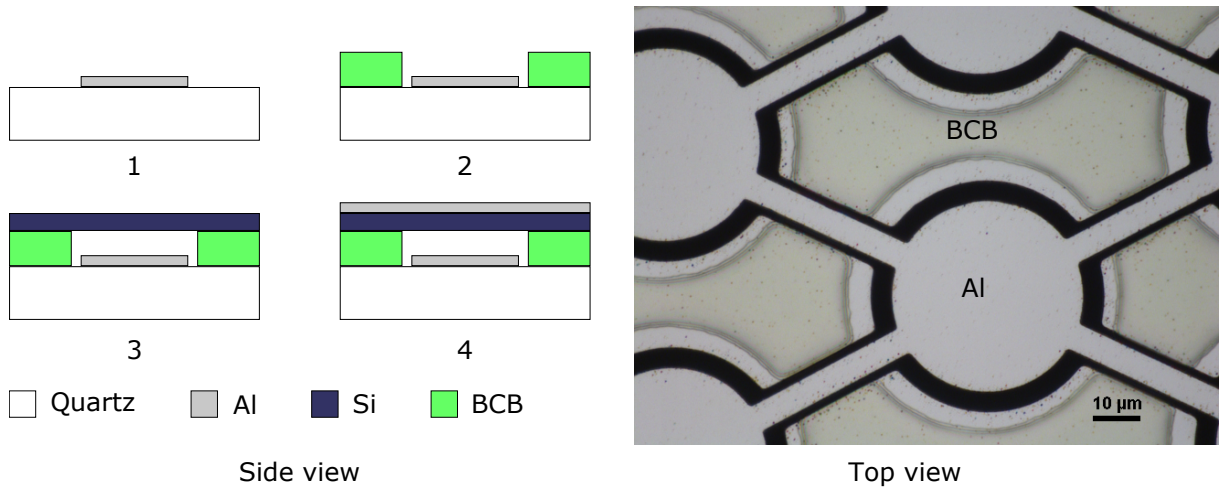


Figure 1: Left figure: Fabrication sketch. 1) Structuring the bottom electrode on top of a quartz wafer. 2) Patterning BCB around the bottom electrode. 3) Bonding of patterned BCB to a SOI wafer followed by etching of the handle and the BOX of the SOI. 4) Depositing metal as top electrode. Right figure: Microscope image of the presented structure corresponding to step 2 in the fabrication sketch. It should be noticed that the BCB never crosses the bottom electrode.

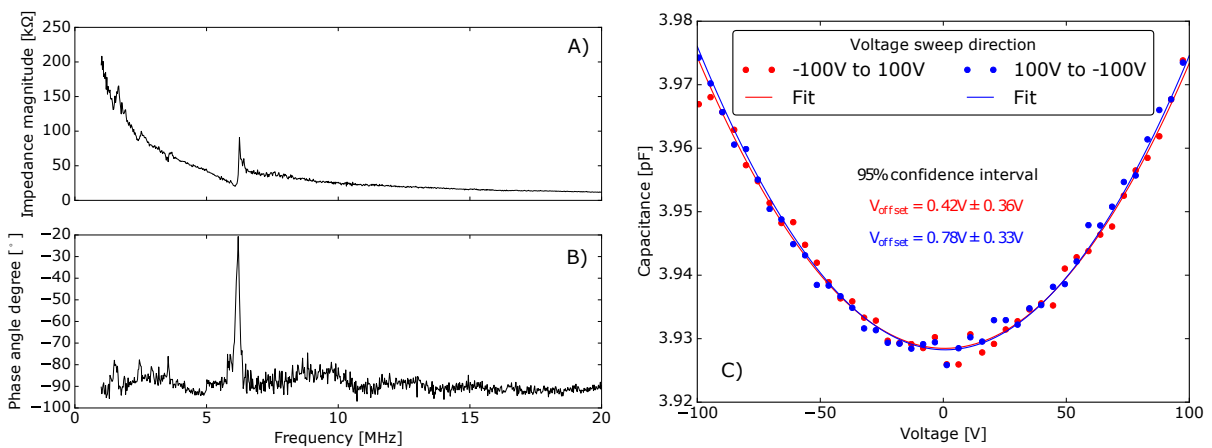


Figure 2: Impedance and CV measurements of the device. Figure A) and B) show the impedance magnitude and phase angle respectively. A resonant peak of the CMUT is observed at 6 MHz. CV measurements are found in Figure C) where the expected parabolic profile from equation (1) is observed.

[1] Zhenhao Li et. al, (2016). Fabrication of capacitive micromachined ultrasonic transducers based on adhesive wafer bonding technique. Journal of Micromechanics and Microengineering, vol 26 issue 11.

[2] Manwar R, Chowdhury S (2016), Characterization of adhesive wafer bonded CMUTs realized from BCB based sealed cavity, Proceeding - IEEE International Symposium on Circuits and Systems, Volume 2016.

Pad printing as an enabling technology for capacitive transducer manufacture

James T. Andrews¹, Andrew Tweedie², Richard L. O'Leary¹

¹Dept. of Electronic and Electrical Engineering, University of Strathclyde, Glasgow, Scotland, UK

²PZFlex, Glasgow, United Kingdom

Capacitive ultrasonic transducers (cUT) comprise a substrate patterned with a regular array of uniformly dimensioned cavities above which a membrane is positioned. Micropatterning of polymer substrates has been shown to be effective methodology for the manufacture of such cUT has recently been demonstrated [1, 2] using a positive mask deposited via pad printing. Since the substrate is a polymer material, an additional step to electrode the substrate is required prior to packaging with a membrane. In the paper micropatterning of conductive substrate is explored via pad printing of a sacrificial pattern onto an aluminium substrate.

The printing pad is manufactured using 3D printing technique, an example pad is illustrated in Figure 1 – essentially the pad comprises an array of styli. The lateral dimensions and spatial distribution of the styli are expected to be replicated via the pattern of droplets deposited by the printing pad. The individual styli are cylindrical with planar tips. The print medium is an alcoholic solution of polyethylene glycol (PEG), a lint free blotter is loaded with a known volume of the PEG solution and the printing pad is used to deposit a pattern onto the aluminium substrate. Once solvent in the printed droplets is allowed to evaporate leaving solid pseudo-cylindrical drops of PEG on the aluminium, these are then over-coated with a UV curing polymer deposited to the height of the PEG using a doctor blade – this is then exposed to UV light to cure the film. The PEG droplets can then be washed out of the UV cured film using deionised water in order to expose the aluminium substrate, resulting in a thin dielectric polymer film comprising an array of cavities, Figure 2. This can then be packaged with a membrane in order to create capacitive transducers.

Single element air coupled devices operating with a nominal centre frequency of 300kHz have been constructed and evaluated experimentally. Transducer bandwidths in excess of 100% were observed with two-way insertion loss of 60dB being typical. Laser vibrometry confirms uniform surface dilation of the excited membrane.

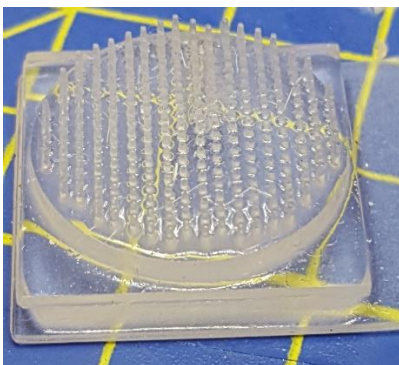


Fig. 1. Photograph of example print pad



Fig. 2. Photograph of micropatterned aluminium substrate

References

- [1] O'Leary, R.L. "Gas coupled polymeric capacitive transducers via pad printing" Proceedings 2015 IEEE International Ultrasonics Symposium, 2015
- [2] O'Leary, R.L. and Harvey, G. "Polymeric capacitive transducers and arrays for gas coupled operation" Proceedings of 2014 IEEE International Ultrasonics Symposium, pp. 177-180, 2014

“Pipe Organ” Air-coupled Broad Bandwidth Transducer

Botong Zhu¹, Benjamin Tiller¹, Alan J. Walker³, James F.C. Windmill¹,
Anthony J. Mulholland²

¹Centre for Ultrasonic Engineering, University of Strathclyde
Glasgow G1 1XW, United Kingdom

²Department of Mathematics and Statistics, University of Strathclyde
Glasgow G1 1XH, United Kingdom

³School of Science and Sport, University of the West of Scotland
Paisley PA1 2BE, United Kingdom

Air-couple transducers can be used to conduct fast non-contact inspection for some special materials in NDT. Normally, the bandwidth of a conventional transducer can be enhanced but at a cost of sensitivity. However, low sensitivity is very disadvantageous in an air-coupled device. This project presents a methodology for improving the bandwidth of an air-coupled micro-machined ultrasonic transducer (MUT) without sensitivity loss by connecting a number of resonating pipes of various length to a cavity in the backplate (as in figure 1(a)). The design is inspired by the pipe organ musical instrument, where the resonant frequency (pitch) of each pipe is mainly determined by its length.

The design, manufacture and experiment can be divided into five steps: Firstly, a fast 1D (in space) mathematical model is employed to ascertain the location of resonances which are from different length of pipes and investigate the benefits of an increased number of pipes. Secondly, a slow but more accurate 3D finite element model provides the optimized parameters of the transducer. Thirdly, a CAD model is built and a commercial 3D printer is used to print the “pipe organ” backplate (as in figure 1(b)). Fourthly, a passive Kapton diaphragm is attached onto the backplate. Finally, a 2D laser vibrometer is used to measure the average velocity of the membrane when applying an external sound source to estimate the bandwidth.

The average velocity of the Kapton membrane in the “pipe-organ” transducer is compared against the standard “cavity-only” transducer. It is found that the velocity bandwidth can be increased with the addition of pipes emanating from the cavity (as in figure 1(c)). A common noise floor was defined for both devices as 6dB below the maximum average velocity of the pipe backed device. The bandwidth of this new device was 2.3 times larger. Further work is now underway to change the passive diaphragm to an active Polyvinylidene fluoride (PVDF) diaphragm. This will allow the bandwidths of the transmission voltage response and the receiving voltage response to be calculated and compared with that of the standard device.

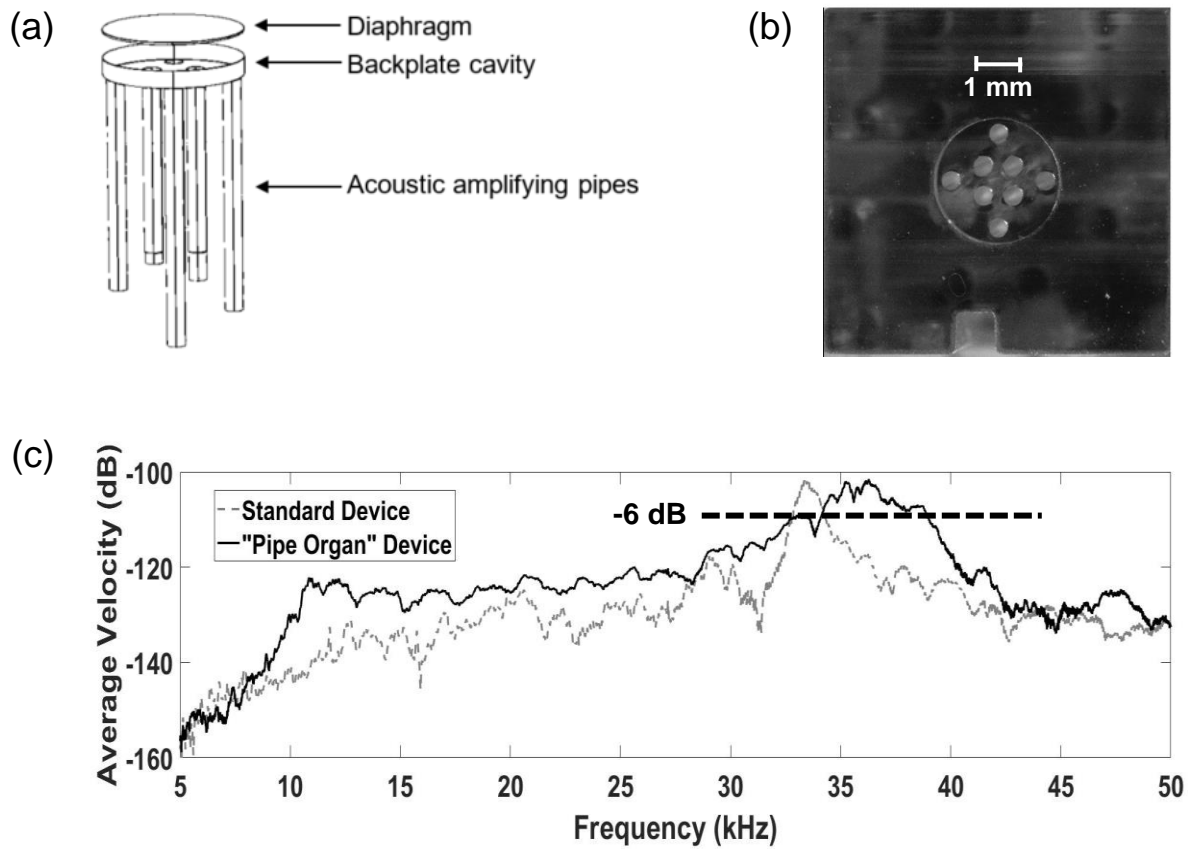


Figure 1, Pipe Organ Transducer. (a) Schematic of pipe organ backplate. (b) Top view of 3D printed backplate. (c) Passive bandwidth increase of diaphragm.

Combined colorimetric and gravimetric CMUT sensor for detection of phenylacetone

Mathias J. G. Mølgaard, Milan Laustsen, Ida L. Thygesen, Mogens H. Jakobsen and Erik V. Thomsen

DTU Nanotech, Technical University of Denmark, Kgs. Lyngby,
Denmark, migmol@nanotech.dtu.dk

Background, Motivation and Objective

Detection of phenylacetone is of interest as it is used as a precursor for the synthesis of (meth)amphetamine. The ability to detect illegal drugs at e.g. border crossings is valuable for governments. Capacitive Micromachined Ultrasonic Transducers (CMUTs) have previously been used to detect small amounts of analyte [1][2]. If the sensitivity of the CMUT is known, the resonance shift can be used to directly calculate the added mass and hereby the amount of an analyte. This typically requires a selective functionalization layer on top of the CMUT in order to differentiate between analytes. However, for some analytes such a layer can be difficult or impossible to obtain.

In this work we use a colorimetric dye, which is selective towards phenylacetone, in conjunction with a CMUT to detect and quantify the analyte.

Statement of Contribution/Methods

CMUTs were fabricated using a single Local Oxidation of Silicon (LOCOS) process to define the cavities on a highly doped Si substrate wafer. The plate is a tensile stressed Si_3N_4 layer bonded to the substrate wafer. The CMUTs have a resonance frequency of 36 MHz in air and an experimentally determined sensitivity of 23 zg/Hz/ μm^2 .

To track the resonance frequency, the CMUTs are via a custom-made PCB connected to a lock-in amplifier (Zurich Instruments, HF2LI) with a built-in phase-locked loop. Colorimetric dye is deposited on the plate of the CMUTs using a spotter. When the analyte adsorbs or is absorbed in the dye a resonance shift is detected due to the increased mass on the plate.

An array of different dyes is spotted on a white paper-like substrate. The presence of an analyte will for some of the dyes result in a color change. These changes are recorded by a digital camera. A specific analyte has a unique set of dyes which will change color and phenylacetone can therefore be distinguished from e.g. water and ethanol.

Results, Discussion and Conclusions

Figure 1 shows the frequency shift as a function of time for an uncoated CMUT and a CMUT coated with the dye DAB4 when exposed to phenylacetone. The frequency shift of the coated CMUT is seen to be larger than for the uncoated CMUT. Figure 2 shows part of the dye array where the first and last photograph has been subtracted, hereby showing the color change due to the analyte. The combination of color changes shown in the figure is specific to phenylacetone.

In conclusion, colorimetric arrays were used to identify phenylacetone while CMUTs were used to quantify the amount, corresponding to a maximum added mass of 25.4pg at the largest frequency shift of ~12kHz.

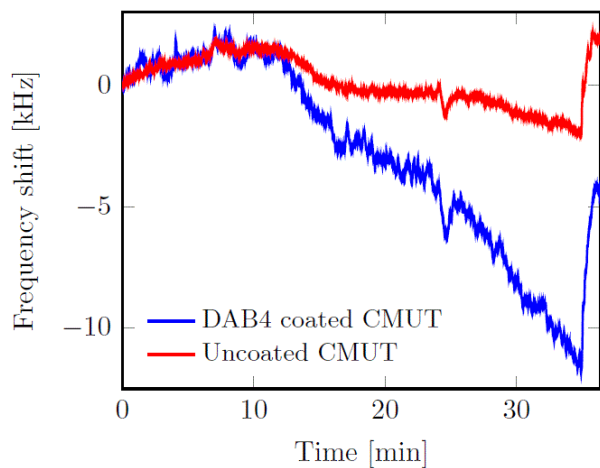


Fig. 1. Frequency shift as a function of time for a CMUT coated with DAB4 and an uncoated CMUT.

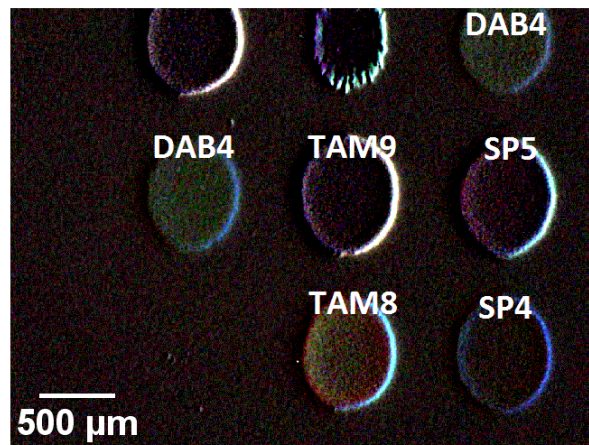


Fig. 2. Result of subtracting photographs of the colorimetric array before and after exposure to phenylacetone.

References

- [1] Lee, H. J., Park, K. K., Kupnik, M., Oralkan, O., & Khuri-Yakub, B. T. (2011). Chemical Vapor Detection Using a Capacitive Micromachined Ultrasonic Transducer. *Analytical Chemistry*, 83(24), 9314–9320.
- [2] Barauskas, D., Pelenis, D., Virzonis, D., Baltrus, J. P., & Baltrusaitis, J. (2016). Greenhouse Gas Molecule CO₂ Detection Using a Capacitive Micromachined Ultrasound Transducer. *Analytical Chemistry*, 88(13), 6662–6665.

Feasibility of interstitial MR-guided high intensity ultrasound heating with CMUTs: *in-vivo* study in pig brain

W. Apoutou N'Djin¹, Jérémy Vion¹, Loïc Daunizeau¹, Christopher Bawiec¹, Guillaume Bouchoux^{1,2}, Nicolas Sénégon³, Jean-Yves Chapelon¹, Alexandre Carpentier²

¹Inserm, U1032, LabTAU, Lyon, F-69003, France ; Univ Lyon, Université Lyon 1, Lyon, F-69003, France

²CarThera Research Team, Brain and Spine Institute, Pitié Salpêtrière Hospital, Paris, 75013, France

³Vermon SA, Tours, 37038, France

apoutou.ndjin@inserm.fr

To date, biomedical Capacitive Micro-machined Ultrasound Transducers (CMUTs) have been mainly developed for imaging purposes and very few studies have proposed this technology for developing therapeutic applications [1-3]. But this technology has a potential for generating high intensity ultrasound, which could have an interest in developing ultrasound thermal ablation therapies. The last decade, however, the feasibility for generating high intensity ultrasound with CMUTs has only been described in a few modeling and *in-vitro* studies [4-6]. The use of CMUTs in continuous wave (CW) mode of operation remains indeed challenging since it requires improving the robustness of cell structures and developing dedicated driving strategies. In the presented study, the feasibility of generating directional ultrasound-induced heating and thermal damage in brain tissue is investigated, with CMUTs designed for interstitial high intensity contact ultrasound (HICU) applications under magnetic resonance (MR) guidance.

Two versions of HICU prototypes were designed and fabricated using a series production batch of wafer bonding CMUTs. An intermediary prototype was made of five 1D-linear arrays (4 elements per array; element size: 2.7 mm x 0.8 mm; elements electrically coupled 2 by 2) mounted side by side on the tip of a 16-cm long, 5-mm wide flat rigid PCB. A final HICU prototype was a multi-faceted catheter incorporating ten 1D-linear arrays, 32.4 mm long and 0.8 mm wide. The arrays were mounted at the tip of a cylindrical 9-French flexible catheter (20-cm long), and formed a prism-shaped 2D array for multidirectional radial HICU exposures. CMUT prototypes were used in a porcine model for generating HICU heating and thermal ablations in brain tissue interstitially. Preliminary numerical simulations allowed identifying a range of surface ultrasound intensities (I_{ac}) suitable for inducing thermal ablation in brain tissues with these CMUT designs ($I_{ac} > 10 \text{ W}\cdot\text{cm}^{-2}$). CMUTs were used in CW mode (HICU sequence: 4s ON/ 1s OFF, $f = 7.9 \text{ MHz}$), and the bias and driving voltages were chosen in order to operate in the collapse-snapback regime and reach the intensity level required for thermal HICU ablation. Ultrasound exposures conditions were

applied through an escalation dose process (total exposure time: from 3 to 15 min, up to 10 active CMUT elements). HICU-induced thermal heating generated with CMUTs was evaluated *in vivo* on 10 pigs and monitored under real-time multi-planar magnetic resonance thermometry (MRT).

Overall, the CMUT prototypes developed in this study allowed generation of HICU exposures *in vivo* and were compatible with the MR environment. Directional HICU-induced temperature increases could be monitored *in the* porcine brain with excellent time-space resolution beyond a radius of 1 mm around the CMUT device (12 MRT maps every 1s, temperature standard deviation: $\pm 2.5^{\circ}\text{C}$). Heating patterns extended over 1 cm from the CMUT elements within 2 min exposures. HICU exposures could be performed continuously without a water-circulating cooling system. The temperature of the brain tissue increased locally above the 55°C threshold necessary for the creation of irreversible thermal damage ($\Delta T_{max} > 35^{\circ}\text{C}$ after 6 min,). Treatment volumes $> 1.5\text{ cm}^3$ could be completed within 13 min. Tissue changes were visible just after treatment on T1- and T2-weighted anatomical images. Tissue ablation boundaries, hypo and hyper signal boundaries respectively detected on T1w and T2w images, correlated well with the 55°C isotherm boundaries (MRT maps). Several contrasts were observable on MR images within the lesion area, which were consistent with previous studies reporting the presence of coagulation and liquefaction necrosis in brain after high intensity ultrasound exposures. Gross sample and histological analyses confirmed the presence of brain tissue coagulations.

The feasibility of using CMUTs for HICU therapy has been shown *in vivo*. Further investigations are ongoing to improve the robustness of the CMUT devices and increase the treatment volumes. This project was supported by CarThera, the French National Research Agency (ANR, 2010) and Single Interministerial Fund (FUI, 2013).

References

- [1] Jin X, Oralkan O, Degertekin FL and Khuri-Yakub BT. Characterization of one-dimensional capacitive micromachined ultrasonic immersion transducer arrays. *IEEE Trans. Ultrason. Ferroelect. Freq. Contr.* 48(3), 750-760, 2001
- [2] Oralkan O, Ergun AS, Cheng CH, Johnson JA, Karaman M, Lee TH and Khuri-Yakub BT. Volumetric ultrasound imaging using 2-D CMUT arrays. *IEEE Trans. Ultrason. Ferroelect. Freq. Contr.* 50(11), 1581-1594, 2003
- [3] Gross D, Coutier C, Legros M, Bouakaz A, and Certon D. A cMUT Probe for Ultrasound-guided Focused Ultrasound Targeted Therapy. *IEEE Trans. Ultrason. Ferroelect. Freq. Contr.* 62(6), 1145-1160, 2015
- [4] Wong SH, Watkins RD, Kupnik M, Pauly KB, Khuri-Yakub BT. Feasibility of MR Temperature Mapping of Ultrasonic Heating from a CMUT. *IEEE Trans. Ultrason. Ferroelect. Freq. Control.* 55(4), 811-818, 2008
- [5] N'Djin WA, Canney M, Meynier C, Chavrier F, Lafon C, Nguyen-Dinh A, Chapelon JY, and Carpentier A. 1D multi-element CMUT arrays for ultrasound thermal therapy. *AIP Conf Proc of the ISTU 2014.* 1821, 050002, 2017
- [6] Farhanieh O, Sahafi A, Roy RB, Ergun AS, and Bozkurt A. Integrated HIFU Drive System on a Chip for CMUT-Based Catheter Ablation System. *IEEE Trans Biomed circuits systems.* Epub ahead of print, 2017

Recent Advancements on the Development of CMUT Probes for 2D and 3D Medical Ultrasound Imaging

Alessandro Stuart Savoia, Barbara Mauti, Giosuè Caliano

Department of Engineering, Roma Tre University, Rome, Italy,
alessandro.savoia@uniroma3.it

Capacitive Micromachined Ultrasonic Transducers (CMUTs) have nowadays reached technological maturity, representing a valid alternative to piezoelectric transducers in medical ultrasound imaging applications, offering larger bandwidth and better thermal efficiency at the expense of an intrinsic nonlinearity. As compared to piezoelectric technology, MEMS technology employed for CMUT fabrication provides increased compatibility with 3D packaging methods, enabling the possible development of advanced transducer-electronics multi-chip modules (MCM) for medical imaging applications. In the last years, research at the Acoustoelectronics Laboratory (ACULAB) of Roma Tre University focused both on the microfabrication technology, for the optimization of the efficiency and reliability of CMUT arrays, and on 3D-packaging methods, for the integration of 2D CMUT arrays with front-end electronics.

In this paper, we present the development of three CMUT probes. The first is a 256-element, 7MHz linear probe, optimized in terms of electromechanical conversion efficiency and long-term reliability using an improved microfabrication process. The improved process features a convenient metallization patterning, aimed at avoiding any superposition of the two electrodes outside the CMUT cavity areas in order to reduce the parasitic capacitance, and the introduction of high quality SiO₂ thin layers between the CMUT electrodes and the Si_xN_y passivation layers, in order to reduce charge injection phenomena. The developed probe is provided with an in-hand 256-channel RX electronics using ultra-compact, low-noise and low-power amplifiers [Fig.1(a)]. The second is a 120+120-element, 7MHz crisscross 2D probe, consisting in two orthogonal overlapped 1D arrays, where all the elements are simultaneously and individually accessible. The developed probe is equipped with an in-hand 240-element RX electronics and with a dynamically reconfigurable high-voltage biasing electronics that allows the implementation of Fresnel focusing in both azimuth and elevation directions [Fig.1(b)]. The third, currently under development, is a 256-element 2D probe based on a Fermat's spiral sparse array configuration. The new probe head is achieved by hybrid 3D-integration of a CMUT 2D array and a 256-channel analog front-end ASIC containing TX pulsers, a TX beamformer and RX amplifiers. An acoustically optimized 3D-packaging method for the interconnection of 2D CMUT arrays and front end ASICs using a wafer-level compatible process has been developed. The entire 3D-integration and packaging has been carried out (Fig.2) on dummy CMUTs and ASICs, i.e. actual-sized chips provided only with one metal layer and electrical interconnection pads, and electrical measurements have been performed successfully to monitor the electrical and mechanical stability of the MCM during the entire packaging process.

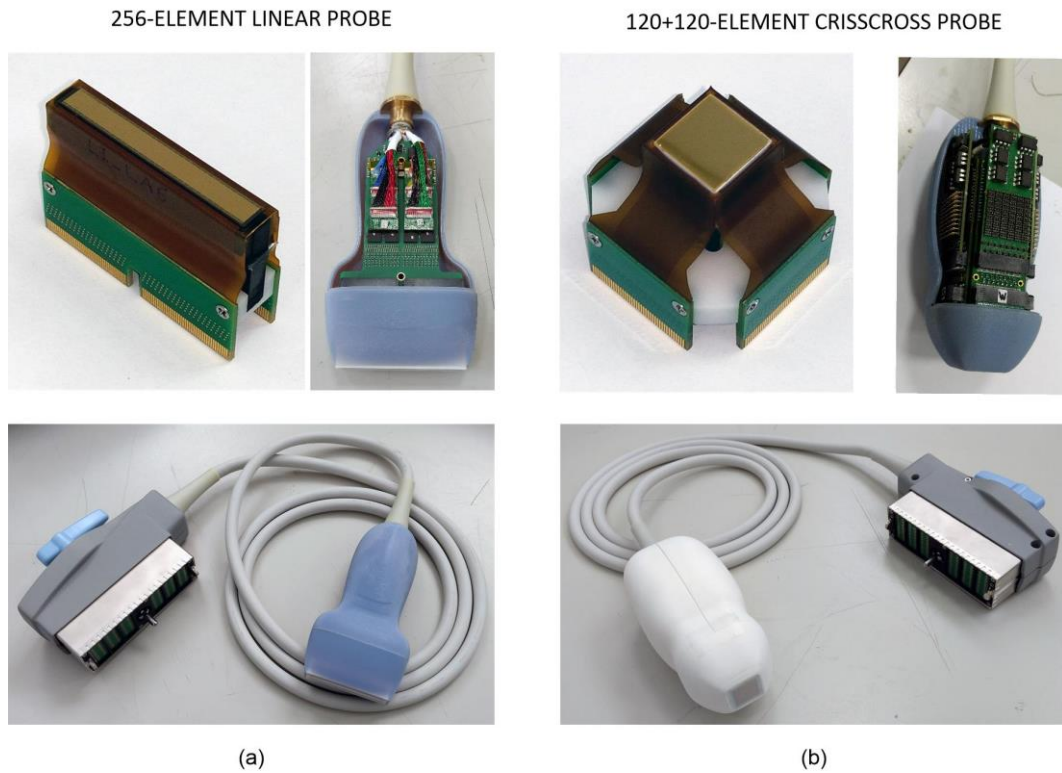


Fig. 1. (top) CMUT probe heads and in-hand electronics, and (bottom) fully packed 256-element linear (a) and 120+120-element crisscross (b) probes.

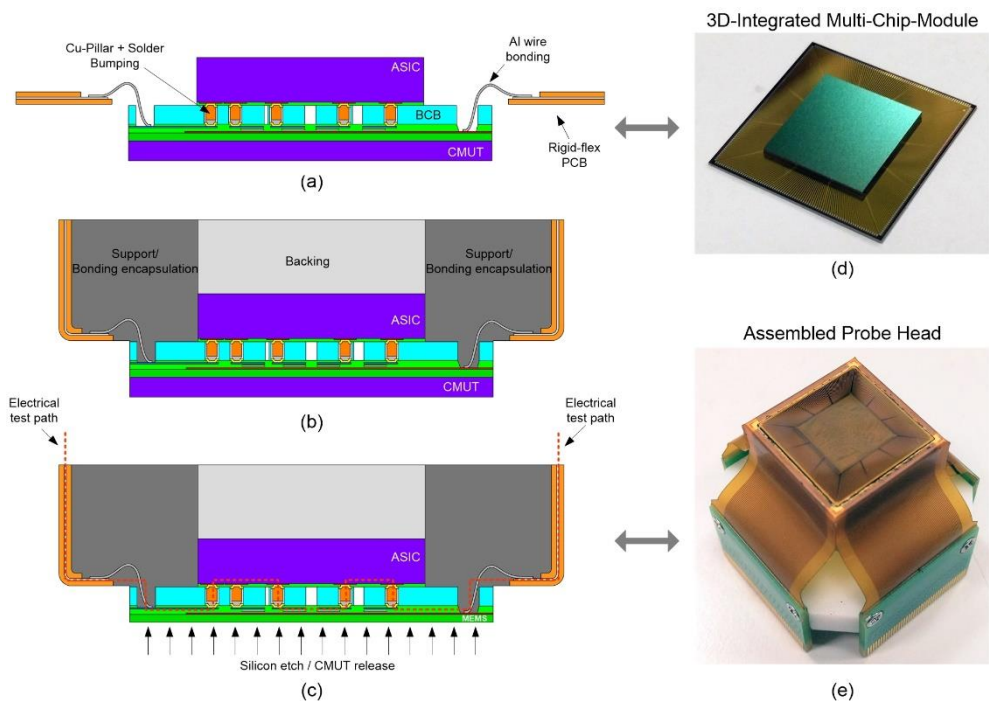


Fig. 2. The developed packaging method uses Cu pillars and solder reflow for electrical interconnection, and patterned Benzocyclobutene (BCB) for mechanical bonding (a). MCMs have been assembled using a chip-to-chip bonding approach (d). A dummy probe head has finally been assembled by connecting the MCM to a rigid-flex PCB and by etching the dummy CMUT silicon substrate (e).

Investigation of a planar 64-element CMUT truncated annular phased array for creating thermal lesions in biological tissue

C. Bawiec^a, W.A. N'Djin^a, G. Bouchoux^a, N. S n gond^b, N. Guillen^c,
J.Y. Chapelon^a

^a Inserm, U1032, LabTau, Lyon, F-69003, France; Univ Lyon, Universit 
Lyon 1, Lyon, F-69003, France

^b Vermon, Tours, 37038, France

^c EDAP TMS, Vaulx-en-Velin, 69120, France

christopher.bawiec@inserm.fr

Background and Motivation: Prototypes of planar 64-element Capacitive Micro-machined Ultrasound Transducer (CMUT) arrays were investigated for their future ability to produce High-intensity Focused Ultrasound (HIFU) thermal lesions in biological tissues. These arrays are composed of 3 MHz, 64-element annular arrays divided into electrically connected quadrants (quarter rings) that are truncated to reduce the overall width of the probe (~35mm). This design also provides a gap in the center for the introduction of a 7 MHz, 256 element linear CMUT imaging array (Fig. 1). Currently used ultrasound probes for the ablation of the prostate utilize geometrically focused piezo- materials for the therapy (16 rings) with a hole in the center containing a piezo- curvilinear imaging array (128 elements). It is hoped that the final implementations of the CMUT probes investigated here can offer performance advantages in terms of higher resolution imaging, more spatial control over the lesion size, and a reduced volumetric footprint of the probe.

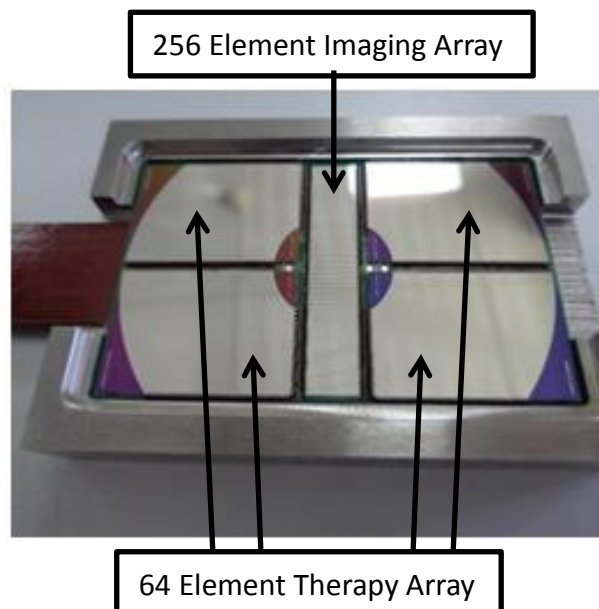


Figure 1 – Photograph of the prototype therapy and imaging array. The dimensions of the CMUT elements are approximately 35 mm by 55 mm.

Methodology: The investigation of this planar CMUT therapy probe was done in both simulation and experimentally. The probe geometry was modelled in Finite Element Method (FEM) software for simulating the pressure field characteristics and also tissue heating parameters (using the bio-heat transfer equation). These simulations enabled determination of the acoustic and temporal parameters necessary to induce thermal lesions in the tissue. The probes capabilities, achievable surface intensity and focusing abilities from 32mm to 72mm, were analysed experimentally. Pressure field measurements were performed in a water tank with a calibrated hydrophone attached to a 3D positioning system and acoustic intensity measurements were performed using the acoustic radiation force balance method. Finally, HIFU exposures have been performed with this prototype in thermally sensitive transparent tissue mimicking hydrogels in order to verify the feasibility of creating focal lesions.

Results: The simulations of the pressure field and the heat deposition demonstrated the feasibility of using this design to create millimetre sized lesions through electronic focusing at depths ranging from 3-7cm in tissue. These simulations provided the necessary surface acoustic intensity (1-10 W/cm²) and timing combination to create a thermal lesion (>55°C) in the tissue within (1-20 sec) at various depths (Fig. 2a). The experimental pressure field measurements also showed that the probe was capable of dynamically focusing from 3-7cm which compared well with the simulated results (Fig. 2b). Finally, the prototype probe was capable of creating visible millimetric sized focal lesions in the tissue mimicking phantom.

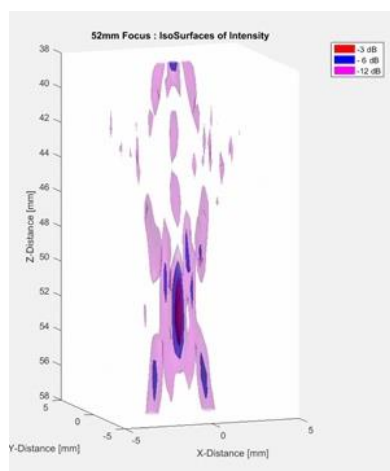


Figure 2a – Hydrophone measured intensity field of 52mm focus in dBs (transducer is at top facing down).

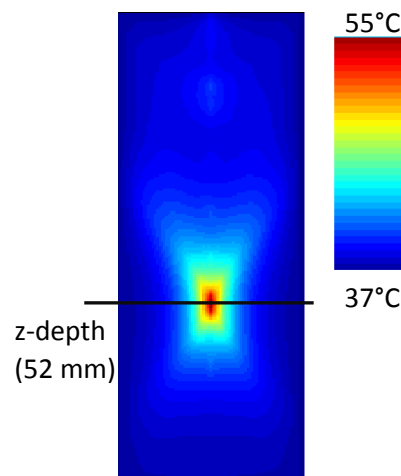


Figure 2b – XZ Simulated heat deposition of 52 mm focussed probe (transducer is at top facing down).

Conclusion: The feasibility of the generating focal thermal lesions in phantom gels has been shown using the planar CMUT annular array probe investigated here. These preliminary results are encouraging for the potential use of this probe for generating thermal lesions in real biological tissues. Yet, there are still many remaining challenges to be overcome regarding the determination of ideal driving parameters, improving efficiency and robustness of the design. This project was supported by the French Single Interministerial Fund (FUI, 2013) and the Whitaker Foundation.

Integrated Receiver Electronics for a CMUT Array

Y. Kansu, C. Bulbul, H. Köymen, A. Atalar

Electrical and Electronics Engineering Department, Bilkent University,
Ankara, Turkey

We describe the receiver electronics suitable for use with a high-frequency CMUT sub-array of 128×2 cells. CMUT cells have a diameter of $40 \mu\text{m}$ with a center-to-center distance of $45 \mu\text{m}$. Signals from the CMUT cells are amplified with a transimpedance amplifier (TIA) for wideband operation. A schematic diagram of the TIA cell is shown in Fig. 1. It uses cascode connected nMOS gain transistors with a cascode connected pMOS current source load to increase the voltage gain and for low-noise operation. An nMOS source follower with a nMOS current source load is used at the output stage [1]. Since the equivalent resistance of CMUT cell is about $200 \text{ K}\Omega$, a transimpedance gain of $400 \text{ K}\Omega$ is chosen, resulting in a feedback resistor, R_f , of $400 \text{ K}\Omega$. A small capacitor, C_f , is added in parallel to satisfy the phase margin requirement. Each of the 128 CMUT cells in the sub-array row has its own TIA to eliminate the loss of an input multiplexer. 128 TIA's share a common bias voltage generator that generates the needed four bias voltages as shown in Fig. 2. The bias generator is designed to reduce the voltage drop on cascode transistors to increase the dynamic range of the receiver.

Only four of the 128 TIA's are active at a given time to limit the power consumption and the number of output connections. Each TIA cell has a pMOS switch to turn on the power and a series nMOS switch to multiplex the output signal. Five digital select lines choose one out of 32 TIA's. The chosen TIA's output signal is fed to a buffer amplifier operating with 5 V supply voltage to be able to drive the coaxial line leading to the beamformer system. The buffer amplifier is built from an operational amplifier using 15 transistors in non-inverting unity gain configuration and has a 40 MHz bandwidth. A block diagram of the whole chip is given in Fig. 3.

Two such chips are used for the 128×2 sub-array. 32 consecutive pulse sequences are needed to probe all cells of the sub-array in a time-multiplexed manner. The whole imaging system consists of 32 such sub-arrays with a total of 8192 elements and it is to be used with a phased-array beamformer system of 256 channels.

The chip is fabricated using $0.35 \mu\text{m}$ analog CMOS process of AMS foundry. TIA cell occupies a space of $45 \mu\text{m} \times 142 \mu\text{m}$ and has a bandwidth of 20 MHz. 128-to-4 line digital decoder circuit is built from four rows of standard cells with a total size of $5768 \mu\text{m} \times 67 \mu\text{m}$. The buffer amplifier has the dimensions of $150 \mu\text{m} \times 170 \mu\text{m}$. Custom designed bond pads are used to increase the density. The complete chip has an area of $6.05 \times 1.14 \text{ mm}$. It consumes 52 mA using a 5 V supply voltage.

Reference:

[1] G. Gurun, P. Hasler, and F. Degertekin, "Front-end receiver electronics for high-frequency monolithic CMUT-on-CMOS Imaging Arrays" IEEE Transactions on Ultrasonics, Ferroelectrics, and Frequency Control, Vol. 58, pp. 2734–2745, 2013.

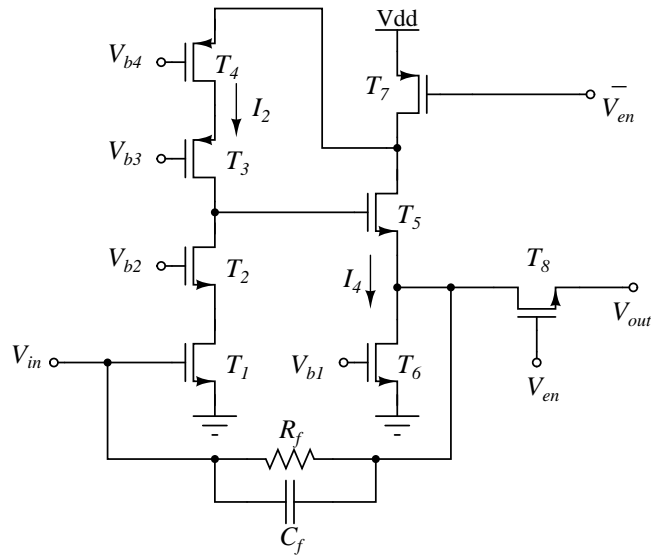


Fig. 1. Schematic diagram of the transimpedance cell.

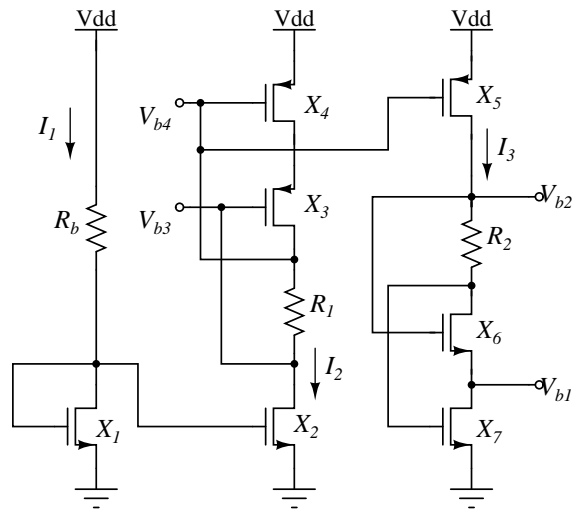


Fig. 2. Schematic diagram of the bias generator.

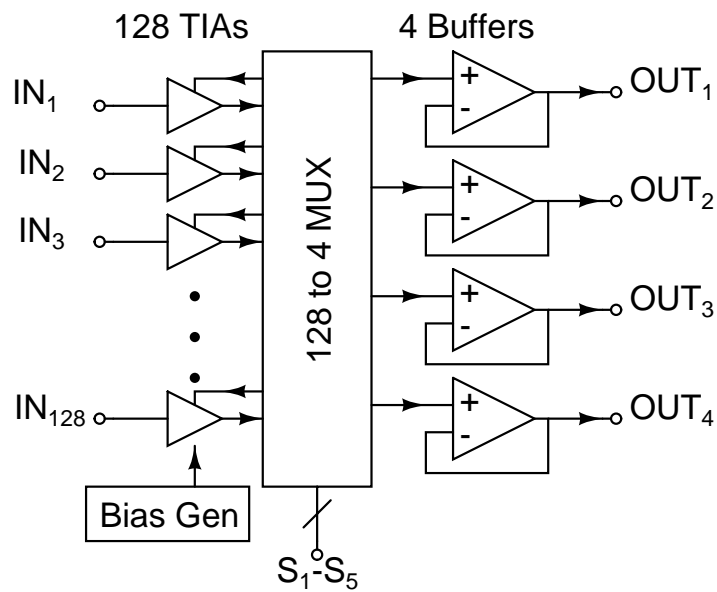


Fig. 3. Block diagram of the receiver chip.

Supply-Doubled Pulse-Shaping Pulser and Supply-Inverted Bipolar Pulser with Tx/Rx Switch for CMUTs

Gwangrok Jung¹, Amirabbas Pirouz¹, Coskun Tekes²,
F. Levent Degertekin^{*1,2}, and Maysam Ghovanloo¹

¹School of Electrical and Computer Engineering, Georgia Institute of Technology, Atlanta, Georgia, USA

²School of Mechanical Engineering at the Georgia Institute of Technology, Atlanta, Georgia, USA

(*corresponding author: levent.degertekin@me.gatech.edu)

A supply-doubled pulse-shaping pulser and a supply-inverted bipolar pulser with Tx/Rx switch are proposed to drive capacitive micromachined ultrasonic transducers (CMUT) in medical ultrasound imaging applications. CMUTs are prone to have low transmit sensitivity. According to large signal CMUT models, this can be remedied with higher pulse voltages and optimized bipolar pulse drives [1]. These circuits are particularly suitable for catheters where interface electronics and transducer arrays are integrated at the tip and lower supply voltages are desired for safety. The proposed pulsers generate output pulse signal with a peak-to-peak voltage that is almost twice the supply level, which improves the driving capability compared to conventional supply-limited pulser, enabling operation at lower supply voltage. Moreover, the added switch is able to protect Rx electronics during the transmit phase. To maximize the transmitted acoustic pressure despite limited transmission capability of the CMUT, we have used a large signal CMUT model to find the optimal three-level pulse and bipolar pulse shapes resulting in higher pressure in the proposed pulser.

A prototype has been implemented in 0.18- μm HV CMOS/DMOS technology with 60 V devices. H-bridge circuit enables charging of off-chip capacitance, C , to drive the supply doubled unipolar pulse and bipolar HV pulse at output (Fig. 1a). The capacitance C , can be implemented on chip as part of the CMUT fabrication process. The negative HV pulse level and the supply-doubled pulse level are defined by the capacitive division between C and CMUT capacitance. Thus, it is key to select proper C based on the output level, slew rate, and power consumption. The proposed pulsers adopt a bootstrap circuit combined with stacked transistors and protection diode, which guarantee HV operation above process limit without lowering device reliability. These circuits generate a supply-doubled three-level pulse and a bipolar pulse, as shown in Fig. 1b, controlled by three low voltage signals and a single HV positive supply. The Tx/Rx switch has a diode-bridge structure with HV protection scheme, enabling integration of the receiver with the bipolar pulser by protecting against the HV signal without adding extra loading.

Measurement results, which are in good agreement with simulations, show that proposed supply-doubled pulser can safely generate up to 85 V_{pp} from 45 V supply (Fig. 2a). Different pulse shapes can be obtained with the three control signals. Changing durations of T_1 , T_2 , and T_3 will affect the width of middle (45 V) and high (85 V) levels. Different pulse shapes affect the acoustic power and frequency content of the ultrasound transmitter, and there is an optimal pulse shape for maximizing the Tx acoustic power for a particular CMUT load. The supply-inverted bipolar pulser can

generate a bipolar pulse of -34.6 to 45 V from 45 V supply voltage with $C = 30$ pF for 8 pF CMUT (Fig. 2b). Using the same supply, simulations show that the pulser is able to drive 2 pF CMUTs up to 85 Vpp. The Tx/Rx switch blocks the HV bipolar pulse, resulting in less than 1.6 V at the receiver input, allowing safe Rx operation.

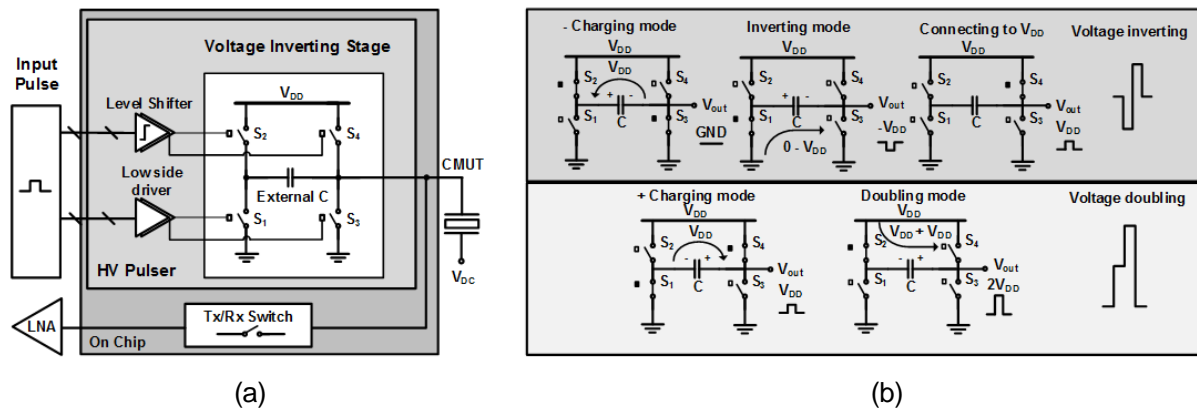


Fig. 1. (a) Simplified schematic diagram of the proposed pulser and Tx/Rx switch. (b) Operation of the voltage inverting stage and voltage doubling stage.

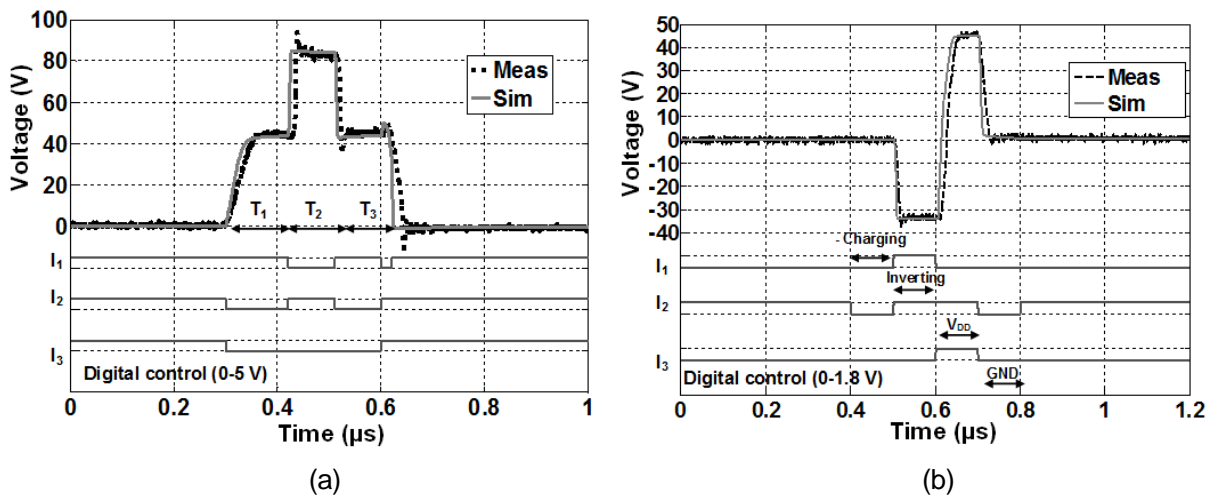


Fig. 2. (a) Measured and simulated three-level output pulse along with three input control signals, $C = 100$ pF, CMUT capacitance (C_{CMUT}) = 8 pF, and (b) supply-inverted output pulse with $C = 30$ pF, CMUT capacitance (C_{CMUT}) = 8 pF.

References

- [1] S. Satir, J. Zahorian and F. L. Degertekin, "Transmit optimization of CMUTs in non-collapse mode using a transient array model," *IEEE Ultrasonics Symp.*, pp. 85-88, 2012.

CMOS-Design of a Cascadable Front-End ASIC for CMUT Arrays

Sandro G. Koch, Andreas Weder, Marcus Pietzsch, Andreas Heinig,
Marco Kircher, Mario Grafe, Nicolas Lange, Jörg Amelung

Fraunhofer Institute for Photonic Microsystems (IPMS), Dresden,
Germany,

sandro.koch@ipms.fraunhofer.de

Abstract

Capacitive micromachined ultrasonic transducers (CMUT) offer many advantages over traditionally used piezo-based ultrasonic transducers. Especially the ability to realize miniaturized transducer array enables high resolution imaging in medical and non-destructive testing applications. Within the framework of the ECSEL project “Advanced Distributed Pilot Line of More-than-Moore Technologies” (ADMONT) Fraunhofer IPMS aims to enhance the electronic integration level for its CMUT technology. Here a novel, fully configurable driver and receiver front-end integrated circuit design that has been developed by Fraunhofer IPMS is presented. The developed Back-End-Of-Line (BEOL) technology allows a reliable co-integration of the CMUT element on top of the CMOS front-end circuit.

Driver and Receiver ASIC

To control the pulse generation and enable the readout of the reflected ultrasonic signal, a digitally controlled driver and readout ASIC has been developed. This design is based on the XFab 0.35 μm process with a high voltage option. The circuit consists of a pull-push stage for high voltage pulse generation and a multistage amplification circuitry. The transmission path and the reception path are separated by a protection switch. The system topology, including the external CMUT element is shown in Figure 1.

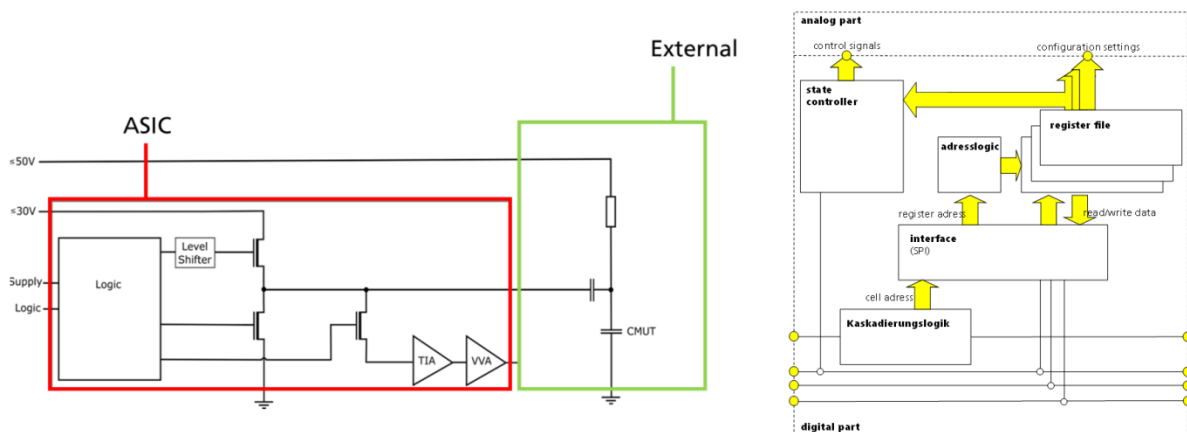


Fig. 1. CMUT transducer system topology (left). Digital ASIC block (right).

The main feature of the front-end ASIC is the complete configurability of all parameters for pulse generation, switching timings and amplification stages, implemented by a digital control block (Figure 1). This concept enables a customizable arrangement and smart control of CMUT arrays, digitally connected

using a shared SPI bus in which each CMUT element is individually addressable and configurable. To reduce hardware complexity on the system level, an intelligent logic for automatic SPI address generation has been implemented. Figure 2 shows the final layout of the front end circuit.

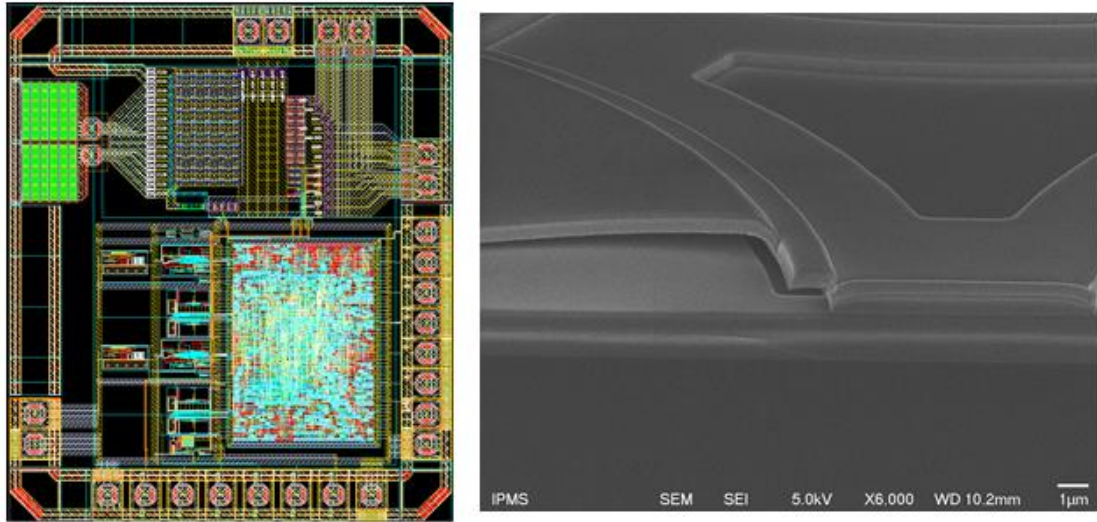


Fig. 2. Layout of the front-end circuit (left). SEM picture of the CMUT structure (right).

Back-End-Of-Line CMUT Technology

At Fraunhofer IPMS a CMOS-compatible sacrificial layer release process for CMUT fabrication is developed during the ECSEL project ADMONT that is suitable for integration as system-in-package and system-on-chip, whereas the monolithic integration onto the state-of-the-art 0.35 μm CMOS process of X-Fab is intended

In order to obtain a reliable long-term behavior of the device, the electrodes are realized with a sputtered amorphous TiAl in the presented case. The bottom TiAl plate is covered with a SiO_2 layer for isolation. During fabrication the cavity is defined by a sacrificial a-Si layer on top of this insulation, which will be released after the upper TiAl plate is deposited (see Figure 2). This technology was improved to realize applications both in gaseous and liquid media.

In a first integration step a single channel CMUT device was co-integrated to the developed ASIC.

The presentation will focus on details of the ASIC design and on recent results of the overall performance of this system.

Simulating CMUT Arrays Using Time Domain FEA

*Mathias Engholm¹, Andrew Tweedie², Søren Elmin Diederichsen¹, Gerald Harvey³,
Jørgen Arendt Jensen⁴, and Erik Vilain Thomsen¹*

¹Department of Micro and Nanotechnology, Technical University of Denmark, Kgs. Lyngby, Denmark

²PZFlex, Glasgow, United Kingdom

³PZFlex, Cupertino, USA

⁴Center For Fast Ultrasound Imaging, Technical University of Denmark, Kgs. Lyngby, Denmark

Finite element method (FEM) has been extensively used for analyzing both static and dynamic behavior of CMUTs. Typical parameters being evaluated include the pull-in voltage, pressure, sensitivity, bandwidth, and crosstalk. PZFlex is a commercial FEA software and has been optimized for the ultrasound industry and is commonly used to design piezo-electric ultrasound transducers. However, PZFlex is not commonly used within the CMUT research field. Nevertheless, it has an explicit modeling approach allowing large structures like CMUT arrays to be modeled and its transient analysis intrinsically supplies non-linear and broadband results from a single run. The objective is to present a multi-element CMUT array model with multiple cells per element and compare the output results to measurements of a fabricated CMUT array.

A 128 element 1D CMUT array is fabricated and assembled in a probe. The individual CMUT cells are circular with a radius of $24.5 \mu\text{m}$ and fabricated using a LOCOS process. The plate is $2 \mu\text{m}$ silicon with 400 nm aluminum on top. The insulation oxide is 400 nm and the vacuum gap is 300 nm . The exact same CMUT cell is modeled in PZFlex using axial-symmetry. The pull-in and the spring softening effect is compared to impedance measurements. To assess the impulse response, bandwidth, output pressure and beam width a 3D CMUT linear array model is presented. The model consists of a central driven element, surrounded by passive elements, with each element containing multiple individual CMUT cells. Symmetry is applied along the elevation direction, significantly reducing model runtime while allowing crosstalk to be observed across multiple adjacent elements.

The figure to the left shows the normalized displacement versus the normalized bias voltage. A transient and a static model is used to calculate the deflection and are compared to an analytic model. The analytic and the static model agree within 2%. In the transient model the inertia of the plate is captured, as the plate does not snap in, predicting a 10 V higher pull-in voltage. The right figure shows the resonance frequency of the transient PZFlex model compared to measurements of a CMUT element. The model agrees with measurements with a difference of less than 3%.

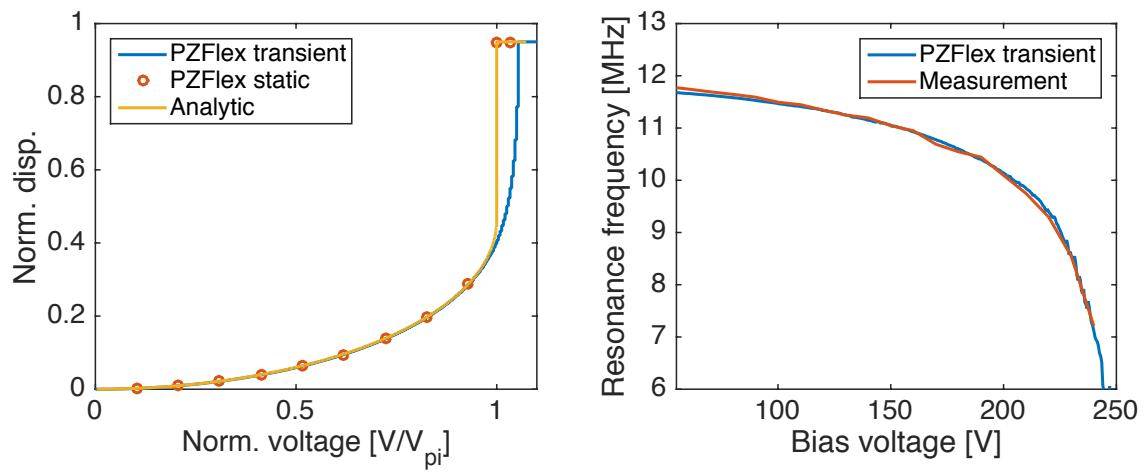


Figure 1: Left: Axial and lateral FWHM of the line spread function measured of the wire phantom. λ was calculated in water with a speed of sound equal to 1480 m/s. Right: SNR on a tissue mimicking phantom with 0.5 dB/(MHz · cm) attenuation without any cyst.

A hybrid boundary element model for the simulation of large PMUT arrays in immersion

Bernard Shieh, Karim G. Sabra, F. Levent Degertekin

G.W. Woodruff School of Mechanical Engineering, Georgia Institute of Technology, Atlanta, GA USA, bshieh@gatech.edu

Piezoelectric micromachined ultrasonic transducers (PMUTs) are a promising technology for the realization of large transducer arrays for use in integrated imaging, sensing, and actuation. It is well established that the dynamics of membrane-type arrays such as PMUTs are strongly influenced by acoustic cross-coupling due to surface waves at the fluid-structure interface, a phenomenon that poses a significant design and modeling challenge [1-3]. Accurate simulation of large arrays—composed of hundreds and thousands of membranes—with standard approaches, such as finite element method (FEM), is impractical due to prohibitive memory and computation requirements. In this work, a hybrid boundary element model is proposed for the transmit simulation of large PMUT arrays in immersion. FEM software (COMSOL Multiphysics) readily handles the simulation of single membrane structures, from which static deformation (stiffness) and harmonic displacement data is extracted. A boundary element method (BEM) formulation based on these inputs handles the membrane-to-membrane acoustic cross-coupling through the calculation of a mutual impedance matrix. For arrays consisting of hundreds of membranes or more, the problem of quadratic storage and cubic time complexity of BEM is avoided by employing a multi-level fast multipole algorithm [4]. We validate this hybrid FEM/BEM method against FEM simulation for both square and circular membranes using a 3x3 matrix array. The model is used to study cross-talk behaviour as well as the impact of electrode coverage for a 5x5 10 MHz matrix array. The large array simulation capability is demonstrated on a 32 element 1-D array with circular PMUT membranes.

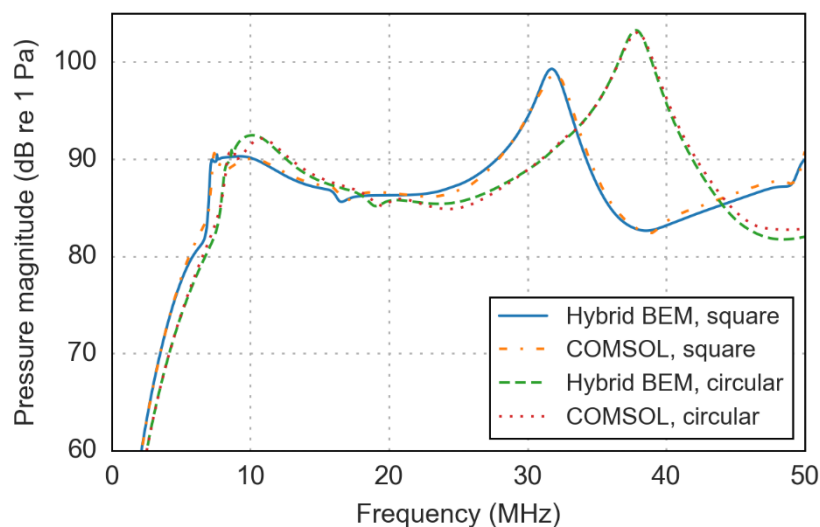


Fig. 1. Comparison of pressure with COMSOL for a 3x3 PMUT matrix array for square ($45 \times 45 \mu\text{m}$) and circular ($60 \mu\text{m}$ radius) membranes. Membranes were composed of $1 \mu\text{m}$ PZT and $2.2 \mu\text{m}$ silicon dioxide layers.

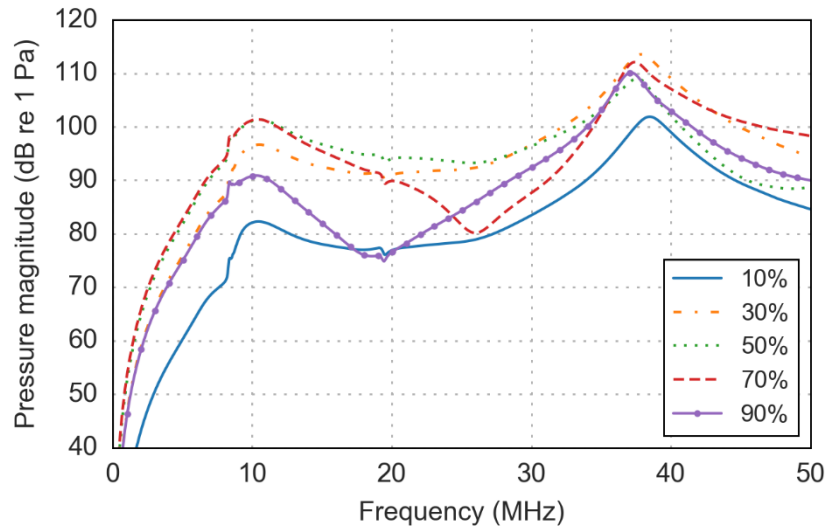


Fig. 2. Electrode coverage optimization for a 5x5 PMUT matrix array.

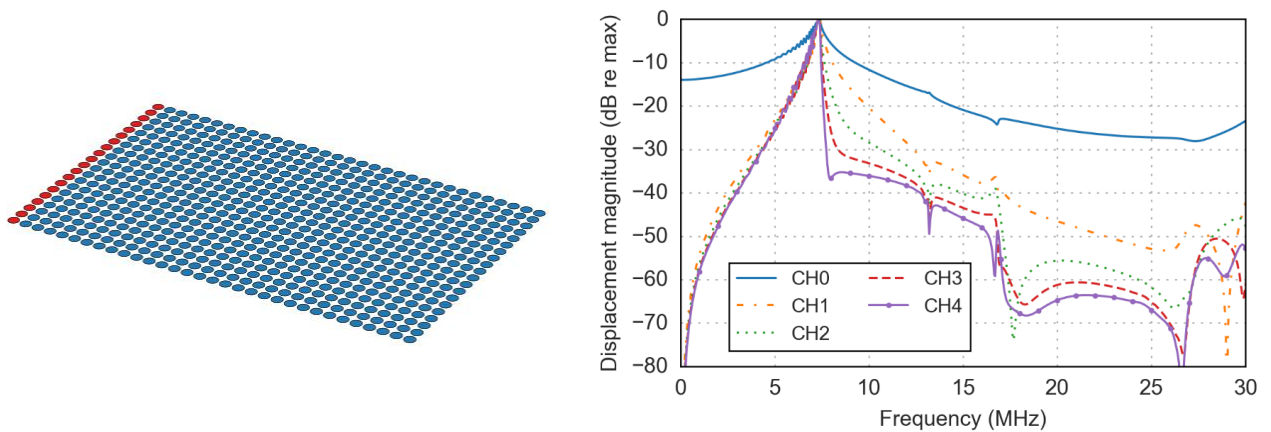


Fig. 3. Geometry of a 32-element linear array (left). Cross-talk response of the first five channels when the first channel is excited (right).

References

- [1] B. Bayram, M. Kupnik, G. G. Yaralioglu, O. Oralkan, A. S. Ergun, D. S. Lin, S. H. Wong, and B. T. Khuri-Yakub, "Finite element modeling and experimental characterization of crosstalk in 1-D CMUT arrays," *IEEE Trans. Ultrason., Ferroelect., Freq. Contr.*, vol. 54, no. 2, pp. 418–429, 2007.
- [2] M. Wilm, A. Reinhardt, V. Laude, R. Armati, W. Daniau, and S. Ballandras, "Three-dimensional modelling of micromachined-ultrasonic transducer arrays operating in water," *Ultrasonics*, vol. 43, no. 6, pp. 457–465, 2005.
- [3] Akhbari, Sina, Firas Sammoura, and Liwei Lin. "Equivalent circuit models for large arrays of curved and flat piezoelectric micromachined ultrasonic transducers." *IEEE Trans. Ultrason., Ferroelect., Freq. Contr.*, vol. 63, no. 3, pp 432–447, 2016.
- [4] B. Shieh, K. G. Sabra, and F. L. Degertekin, "Efficient broadband simulation of fluid-structure coupling for membrane-type acoustic transducer arrays using the multilevel fast multipole algorithm," *IEEE Trans. Ultrason. Ferroelectr. Freq. Contr.*, vol. 63, no. 11, pp. 1967–1979, 2016.

Frequency-Tunability of a Collapse-Mode CMUT: from modelling to pre-clinical imaging

Martin Pekař^{1,2}, Nenad Mihajlović¹, Alexander F. Kolen¹, Harm Belt¹, Jeannet van Rens¹, Frank Budzelaar¹, Bas Jacobs¹, Frank van Heesch¹, Wendy U. Dittmer¹, Debbie Rem-Bronneberg¹, Stephan H. M. van Nispen³, Rob H. B. Fey³, Sergei Shulepov¹, Henk Nijmeijer³, Imo E. Hoefler⁴, Tamas Szili-Török², Hendrik J. Vos^{2,5}, Johan G. Bosch², Gijs van Soest², Nico de Jong^{2,5}, Antonius F. W. van der Steen^{2,5}

¹Philips Research, Eindhoven, the Netherlands

²Erasmus MC, Rotterdam, the Netherlands

³Department of Mechanical Engineering, Eindhoven University of Technology, the Netherlands

⁴Faculty of Veterinary Medicine, Utrecht University, the Netherlands

⁵Dept. of Imaging Physics, Delft University of Technology, Delft, the Netherlands

E-mail: martin.pekar@philips.com

In intracardiac echocardiography (ICE) it might be beneficial to provide ultrasound images acquired at multiple frequencies to provide high resolution and high penetration combined in a single ICE catheter. The objective of the presented work is to investigate the feasibility of a frequency-tunable imaging with a capacitive micromachined ultrasonic transducer (CMUT) operated in a collapse mode.

We have developed a semi-analytic model of collapse-mode CMUT [1]. The modelled collapse-voltage is 59 V. Simulated impulse response predicts center frequency of 12.9 MHz and 16.6 MHz at a bias voltage of 100 V and 160 V, respectively. Experimental validation with a manufactured CMUT prototype [2] shows that the dynamic response and frequency-tunability are modelled with a satisfactory accuracy as shown in Fig. 1.

Further experimental studies show that the center frequency of a collapse-mode CMUT can be controlled between 8 MHz and 15 MHz, if the lower bias voltage range is extended and the driving pulse is optimized. Mechanically-scanned B-mode imaging is performed on a phantom at 8 MHz, 11 MHz, and 15 MHz as a first proof of principle of a frequency-tunable imaging with a collapse-mode CMUT [4].

A 2x2 mm² 32-element phased-array CMUT is integrated with front-end electronics in a rigid probe prototype and connected to Verasonics system (Kirkland, WA, USA) for 2-D real-time imaging and data acquisition [4]. CMUT imaging performance is quantified in terms of resolution and penetration depth at a range of bias voltages, driving pulse frequencies, and number of pulse cycles. Based on this characterization settings for high-penetration, generic, and high-resolution imaging modes are identified. The first 2-D imaging results are shown.

The developed probe prototype is tested *ex vivo* in a passive heart platform [5]. Images of an aortic valve acquired in high penetration (6 MHz), generic (12 MHz), and high-resolution (18 MHz) mode combine satisfying image quality and penetration depth between 2.5 cm and 10 cm as shown in Fig. 2.

Next, the CMUT probe prototype is further miniaturized into a 12-Fr steerable, forward-looking ICE catheter. The ICE catheter prototype is tested *in vivo* using a porcine animal model [5]. Images of an aortic valve are acquired in the three imaging modes with the ICE catheter placed in an ascending aorta at multiple depths. It was found that the combination of the forward-looking design and frequency tuning capability allows visualizing intracardiac structures of various sizes at different distances relative to the catheter tip, providing both wide overviews and detailed close-ups.

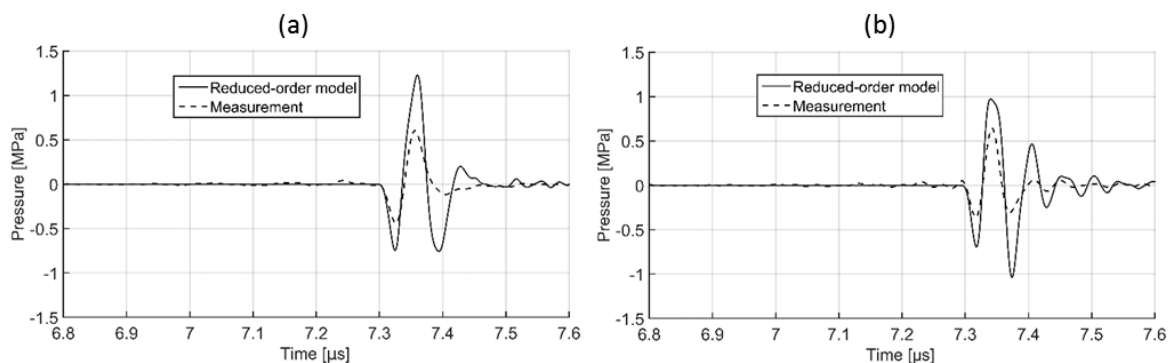


Fig. 1. Modelled and measured impulse response of a fluid-loaded CMUT array at a bias voltage of (a) 100 V and (b) 160 V.

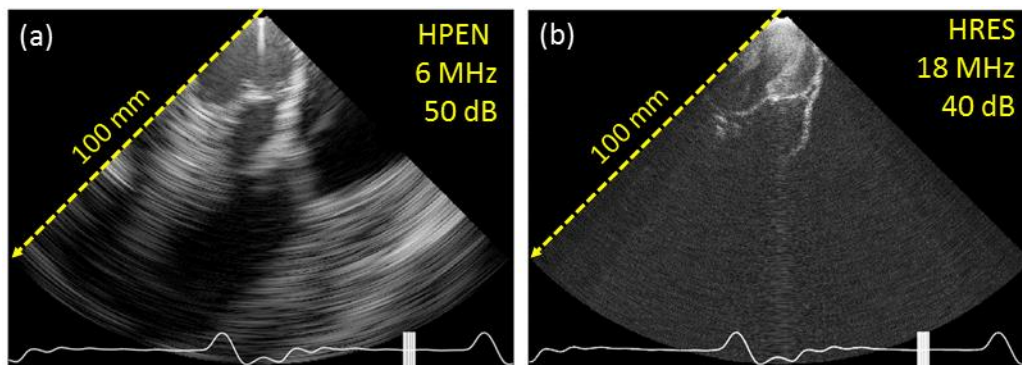


Fig. 2. Long-axis view of aortic valve obtained with the developed frequency-tunable, forward-looking, steerable CMUT catheter prototype *ex vivo*.

References

- [1] Martin Pekař, Stephan H. M. van Nispen, Rob H. B. Fey, Sergei Shulepov, Nenad Mihajlović, Henk Nijmeijer, *Sensors and Actuators A: Physical* (in review).
- [2] Dirksen, P. and Lugt, A. van der (2009), Production of Pre-Collapsed Capacitive Micro-Machined Ultrasonic Transducers and Applications Thereof, Patent WO 2009037655 (A2), March 2009.
- [3] Martin Pekař, Wendy U. Dittmer, Nenad Mihajlović, Gijs van Soest, Nico de Jong, Frequency Tuning of Collapse-Mode Capacitive Micromachined Ultrasonic Transducer, *Ultrasonics*, vol. 74, p. 144-152, 2017.
- [4] Pekař, M., Mihajlović, N., Belt, H., Kolen, A. F., Rens, J. van, Budzelaar, F., Jacobs, B., Bosch, J. G., Vos, H. J., Steen, A. F. W. van der and Rem-Bronneberg, D. (2016) 'Frequency-Agility of Collapse-Mode 1-D CMUT Array', in *Proceedings - IEEE Ultrasonics Symposium*. Tours: IEEE.
- [5] Martin Pekař, Alexander F. Kolen, Harm Belt, Frank van Heesch, Nenad Mihajlović, Imo E. Hoefler, Tamas Szili-Török, Hendrik J. Vos, Johan G. Bosch, Gijs van Soest, Antonius F. W. van der Steen. Preclinical Testing of Frequency-Tunable Capacitive Micromachined Ultrasonic Transducer Probe Prototypes, *Ultrasound in Medicine and Biology* (in press).

The Effect of Insulator Charging on CMUT Performance

Hayrettin Köymen, Abdullah Atalar, Saadettin Güler, İtir Köymen, A. Sinan Taşdelen, and Aslı Ünlügedik

H. Köymen, A. Atalar, and I. Köymen are with the Electrical and Electronics Engineering Department, Bilkent University, Ankara, Turkey (e-mail: koymen@ee.bilkent.edu.tr)

S. Güler and A. S. Taşdelen are with the Bilkent University Acoustics and Underwater Technologies Research Center (BASTA), Bilkent University, Ankara, Turkey (e-mail: sinan@ee.bilkent.edu.tr)

A. Ünlügedik is collaborating with BASTA, Bilkent University, Ankara, Turkey

Capacitive micro-machined ultrasonic transducers (CMUT) consist of two parallel plate electrodes, where one of the electrodes is deposited on a non-moving substrate and the other electrode is placed on a suspended, edge-clamped elastic plate, that are separated by a vacuum or partial atmospheric pressure gap. One or both electrodes are usually covered with an insulating layer that may become polarized or may trap space charges during production processes or under operation conditions. Materials such as silicon dioxide (SiO_2), silicon nitride (Si_3N_4) and aluminium oxide (Al_2O_3) are used as insulators. These insulating materials are also widely used as electrets for their superior charge retaining properties. The mechanisms of polarization and charging/discharging have been studied extensively since the emergence of electrets.

Although the morphology of a CMUT is very similar to capacitive and electret microphones, the fact that the gap is not pressure compensated causes significant differences in their analytical modelling. A pressure difference between the immersion medium and the gap causes a static deflection of the radiating plate. The deflection profile for a circular CMUT in the linear region is given by

$$x(r) = x_p(t) \left(1 - \frac{r^2}{a^2}\right)^2, r \leq a$$

where $x_p(t)$ is the spatial peak displacement at the centre of the plate with radius a .

It is possible to analytically show that the effect of charging can be modelled by adding a series dc voltage source having a value of equivalent electret voltage V_E to the lumped element large and small signal models given in [1]. The large signal *rms* model is shown in Fig. 1. Here, F_{Rb} represents the force due to ambient pressure and $f_i(t)$ is the force due to incident acoustic signal. This lumped effect also minimizes the sensitivity of performance to the non-uniform trapped charge distribution in the insulating layers in radial direction. The new model is energy consistent. CMUT biasing charts are updated according to the charging effect.

The validity of the model is tested with a previously fabricated and charged airborne CMUT cell having a resonance frequency of 103.4 kHz. Impedance measurements are carried out to find the equivalent electret voltage, V_E . Absolute sensitivity measurements are done in air showing that the model prediction is in agreement with the measurements. Also, transient response simulations and measurements are carried out to show that the model predicts the waveform behaviour very well. Fig. 2 is a comparison of model prediction with the measurement. The model is simulated with the transient simulator of ADS [2], a harmonic-balance simulator which can take care of nonlinear as well as frequency-domain specified elements.

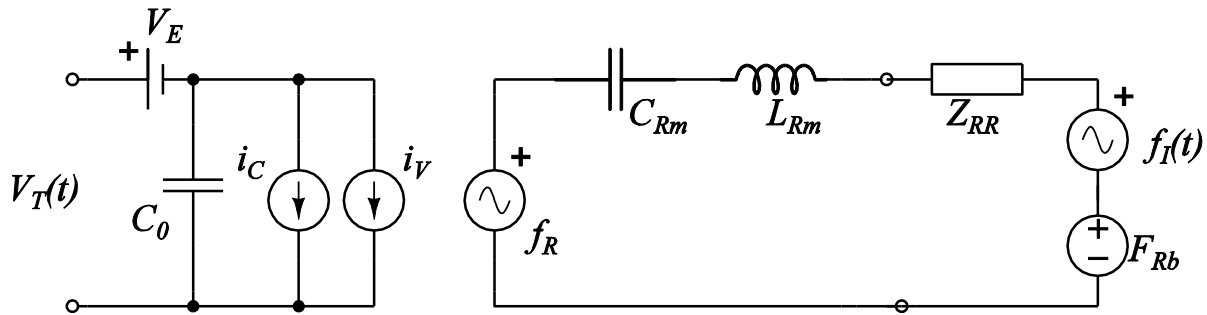


Fig. 1. Large-signal model of a CMUT cell with charging.

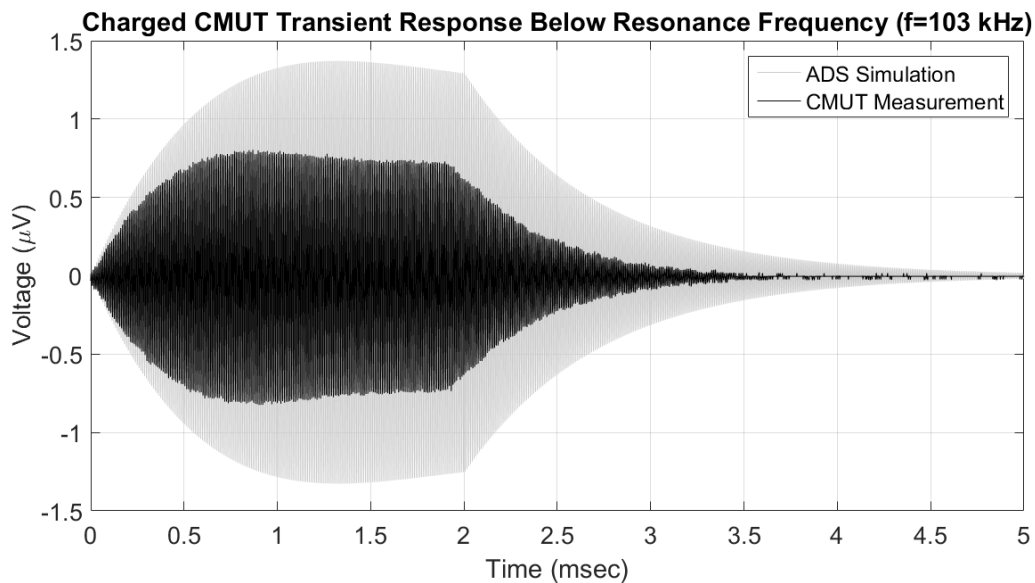


Fig. 2. Comparison of a Single Cell Airborne Charged CMUT Transient Reception Response Model Simulation and Measurement Data

References

- [1] H. K. Oğuz, A. Atalar, and H. Köymen, "Equivalent Circuit-Based Analysis of CMUT Cell Dynamics in Arrays," *IEEE Transactions on Ultrasonics, Ferroelectrics, and Frequency Control*, Vol. 60, pp. 1016–1024, 2013
- [2] Advanced Design System, Keysight Technologies Inc., www.keysight.com

Multiphysics Model and Experimental Validation of an Air-Coupled PMUT at 100 kHz

G. Massimino¹, L. D'Alessandro¹, F. Procopio², R. Ardito¹, M. Ferrera²,
A. Corigliano¹.

¹ Department of Civil and Environmental Engineering, Politecnico di Milano, Piazza Leonardo da Vinci 32, 20133 Milan, Italy.

²Analog, MEMS & Sensors Group, ST Microelectronics, Via Olivetti 2, 20100 Agrate Brianza, Italy.

This work is focused on the multi-physics modelling via finite element method of a 440 μm radius PMUT membrane (Fig. 1) with operating frequency of 100 kHz and PZT thin film active layer, and on its experimental validation. This paper builds up on previous works [1, 2]. In the literature, the most common air-coupled PMUTs have AlN as active layer. Compared to previous works, mainly related to AlN PMUTs with operating frequency above 200 kHz [2-3], this work considers a complete multi-physics modelling, the fabrication residual stresses, their effect on the dynamic response of the device and the thermal-viscous fluid losses appearing in the boundary layer near to the solid and in the bulk air. The numerical model presents the multiple interactions among electrical, mechanical and acoustic fields. To compute the eigenfrequency shift, due to the pre-stress state, a non-linear static analysis is performed, while the thermo-viscous acoustic-structure interaction is activated in the harmonic analysis to estimate the real Q-factor of the vibrating system. Experimental validations are discussed for the initial static deformation, fundamental frequency shift and sound pressure level at 3.5 cm on the vertical axisymmetric axis for the unpackaged transducer. This complete modelling can guide designers through frequency and quality factor control of the device.

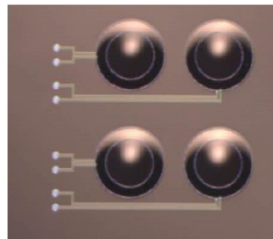


Fig. 1. Optical microscope image of four PMUTs.

The analyzed transducer is a circular fully-clamped diaphragm with radius/thickness aspect ratio of about 55. The PZT thin film is deposited with Sol-Gel technique and it is in circular hat configuration with inner radius equal to 308 μm . The finite element model is built in COMSOL Multiphysics v5.2a; to reduce the computational burden, while including all the possible features during the wave emission phase, the axisymmetric configuration is adopted. The model captures in a proper way the electro-mechanical-thermo-acoustic coupling along with the geometrical non-linearities and runs in 40 minutes with i7 CPU @3.4 GHz and 16 GB RAM for a complete frequency sweep. A proper finite element discretization must be used at the interfaces between solid and fluid where main thermo-viscous fluid losses happen.

The membrane shows a measured initial deflection of 5.5 μm , while the numerical result is 5 μm (Fig. 2, left), the difference is attributed to the uncertainty in the values of the residual stresses. The operating frequency of the device shifts from the theoretical value (without residual stresses) of 111.5 kHz to 99.8 kHz and it is correctly captured by the model which reports 100.2 kHz. Going further in the acoustic domain, the Sound Pressure Level is numerically estimated for the stand-alone unpackaged diaphragm.

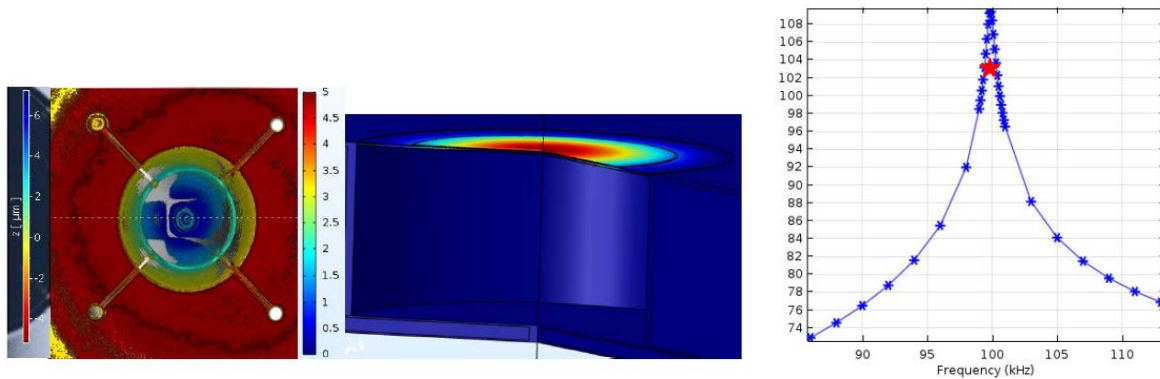


Fig. 2. Initial static deflection due to fabrication residual stresses: experimental measurement by means of Polytec MSA-500, numerically computed (left). Sound Pressure Level [dB] at 3.5 cm on the vertical axisymmetric axis (blue asterisks). numerical experimental result (red star) (right).

The numerical model overestimates the experimental value of 103 dB at 3.5 cm on the vertical axis of symmetry (Fig. 2, right) due to the presence of other sources of losses not considered (i.e. cross-talk between membranes). The device quality factor has been measured by means of the free vibration decay test: $Q_{\text{tot}}=80$ is obtained, while the numerical estimated Q-factor for the fluid losses only (both radiation and thermal-viscous losses), Q_{fluid} , is 190. The boundary layer thickness in the fluid domain is comparable to the thickness of the diaphragm [4]. The sources of structural damping (such as thermo-elastic losses, interface losses, anchor losses) are modelled through an imposed isotropic loss factor equal to $1/Q_{\text{struct}}$ where $Q_{\text{struct}}=140$ applied to the diaphragm [5]. Moreover, the PMUT devices are usually packaged, so the interaction between the surrounding medium does not involve directly the vibrating membrane only but the package as well. Hence, the model has been enriched to take into account the presence of a metallic protecting cap. The numerical procedure has been applied to study the effect of package and to extract a set of design guidelines.

References

1. G. Massimino, L. D'Alessandro, F. Procopio, R. Ardito, M. Ferrera, A. Corigliano, (2016), "Multiphysics analysis and experimental validation of an air coupled piezoelectric micromachined ultrasonic transducer with residual stresses", *Procedia Engineering*, 168, 852-855, 2016.
2. G. Massimino, L. D'Alessandro, F. Procopio, R. Ardito, M. Ferrera, A. Corigliano. Air-Coupled PMUT at 100 kHz with PZT Active Layer and Residual Stresses: Multiphysics Model and Experimental Validation. *Proceedings Eurosime 2017, Dresden*, 3-5 April 2017.
3. D.A Horsley, O. Rozen, Y. Lu, A. Guedes, R. Przybyla, H.-Y. Tang, B.E. Boser, "Pulse-echo ultrasonic fingerprint sensor on a chip", *Proc. SENSORS 2015*.
4. S. Akhbari, F. Sammoura, C. Yang, A. Heidari, D. Horsley, L. Lin, "Bimorph pMUT with dual electrodes", *Proc. IEEE MEMS 2015*.
5. M. Malinen, M. Lyly, (2004), "A Finite Element Method for the Modeling of Thermo-Viscous Effects in Acoustics", *Proc. ECCOMAS 2004*.
6. K. K. Park, H. J. Lee, P. Crisman, M. Kupnik, Oralkan, B. T. Khuri-Yakub, (2008), "Optimum design of circular CMUT membranes for high quality factor in air", *IEEE International Ultrasonics Symposium Proceedings 2008*.

Characterization infrastructure for the CMUT platform

Chris van Heesch, Peter Dirksen, Marco de Wild

Philips Research, Eindhoven, The Netherlands,
chris.van.heesch@philips.com

Philips Research has been developing a CMUT platform during the last 10 years¹, aiming at a wide range of ultrasound transducers for various applications including conventional imaging probes, IVUS & ICE catheters^{2,3}, and potential new applications. The versatility of this platform results in a wide frequency range (1 to 50 MHz) and the sizes of the transducers (~1 mm² to ~25 cm²) that can be designed with the CMUT technology.

This presentation discusses the electrical and acoustical characterization for production volumes, of the order of 10.000 medical grade devices per year and up. Consequently, the infrastructure to characterize the CMUTs also needs to be able to handle this large variety and volume of samples. This presentation gives a detailed description of all the characterization methods of the CMUT devices developed for a fully automatic production process starting from on wafer level process & electrical characterization to acoustic measurements and imaging tests of individual samples. Typical workflows will be described and examples are given on:

Wafer level:

- Processing characterization modules (PCM) analysis to monitor the various processing steps, such as layer thicknesses (Figure 1,a)
- Capacitance vs voltage measurements (CV) of the CMUT to show functionality and determine wafer uniformity (Figure 1,b)
- Impedance measurements to verify resonance frequencies (Figure 2,a)

Transducer level:

- Impedance measurement to verify acoustic stack (window thickness and backing) (Figure 2,b)
- Hydrophone measurement for acoustic performance (Figure 3,a)
- Lifetime measurements (Figure 3,b)
- Interferometry for trouble shooting (Figure 4,a)

System level:

- Ultrasound imaging for system testing and product performance evaluation (Figure 4,b)

The aim of this presentation is to show the tradeoff between accurate, and detailed (acoustical) characterization on transducer level on one side, versus fast and fully automated (on wafer electrical) measurements on the other side. Finally, it will be shown that this infrastructure allows predicting the ultrasound imaging performance based on the CMUT characteristics.

References

- [1] Dirksen, P. and Lugt, A. van der, Production of pre-collapsed capacitive micro-machined ultrasonic transducers and applications thereof, WO 2009037655 A3
- [2] Martin Pekař, Wendy U. Dittmer, Nenad Mihajlović, Gijs van Soest, Nico de Jong, Frequency Tuning of Collapse-Mode Capacitive Micromachined Ultrasonic Transducer, Ultrasonics, vol. 74, p. 144-152, 2017.
- [3] <http://www.incite-project.eu/index.php/publications>

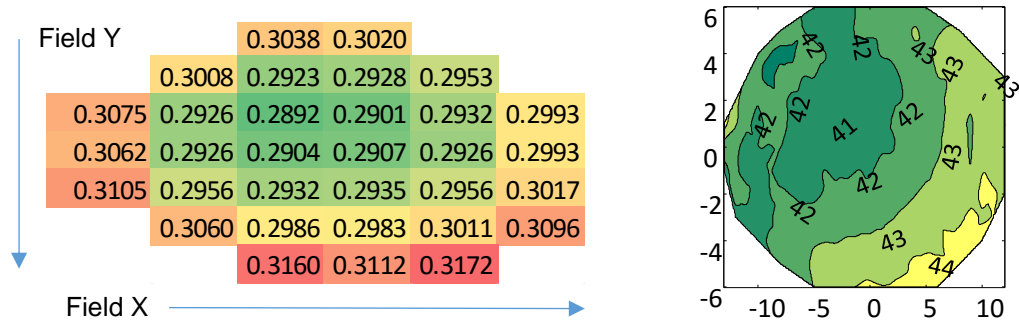


Figure 1) a. Wafer-map of PCM structure data, b. Wafer-map of collapse voltage of all 252 devices

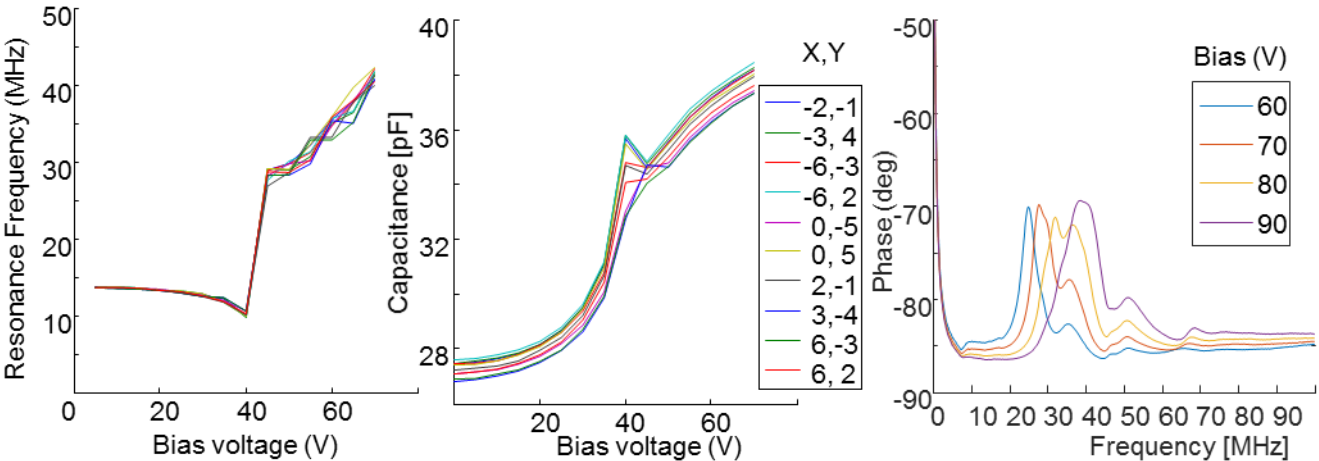


Figure 2) a. & b. Resonance and capacitance determined by electrical impedance on various positions on the wafer, c Phase measurement for various bias voltages for a sample in water.

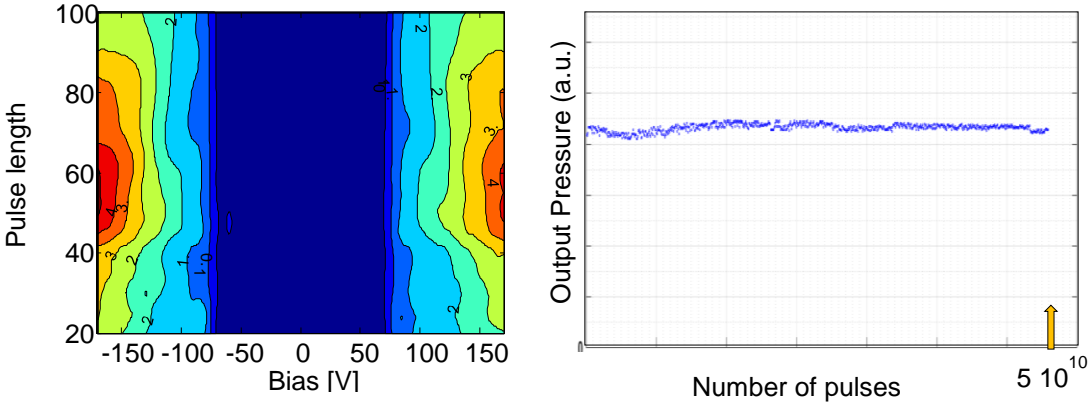


Figure 3) a. Acoustic pressure (in MPa) measurement as function of bias voltage and frequency, b. Lifetime measurement.

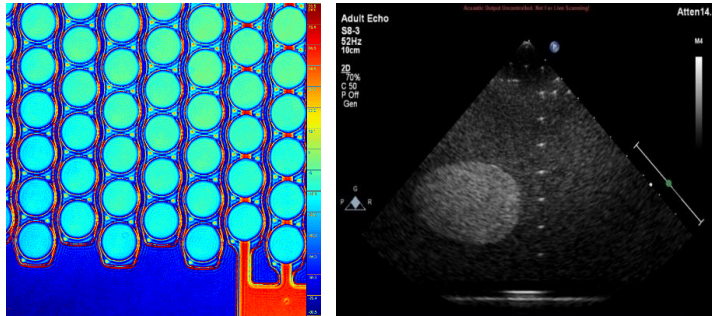


Figure 4) a. Interferometer image of a CMUT array, b. Ultrasound image of a phantom acquired with the developed CMUT probe

Output Pressure and Pulse-Echo Characteristics of CMUTs as Function of Plate Thickness

*Søren Elmin Diederichsen, Jesper Mark Fly Hansen, Mathias Engholm,
Jørgen Arendt Jensen, and Erik Vilain Thomsen*

Technical University of Denmark, 2800 Kgs. Lyngby, Denmark
seldi@nanotech.dtu.dk

The energy transduction of a Capacitive Micromachined Ultrasonic Transducer (CMUT) depends on the movement of a flexible plate, which has a low mechanical impedance compared to its bulky piezoelectric counterpart. Consequently, the output pressure of a CMUT is generally lower. This limits the penetration depth, and thus the visualization of deeper structures in the body, as well as non-linear imaging such as tissue harmonic imaging. The objective of this work is to investigate how the output pressure and pulse-echo signal of a CMUT scales with the (silicon) plate thickness.

The CMUTs are fabricated using two consecutive local oxidations of silicon, followed by direct wafer fusion bonding to a silicon-on-insulator (SOI) wafer [1]. The plate thickness is thereby determined by the SOI wafer device layer thickness. CMUTs with plate thicknesses of 2 μm , 9.3 μm and 15 μm are realized. The cell radii and gap height resulting in an immersion frequency of 5 MHz and pull-in voltage of 200 V are designed using finite element analysis. The fabricated CMUTs are coated with PDMS and mounted in a water tank, where a hydrophone and a plane reflector, respectively, are placed in a distance of 1 cm from the CMUT surface. The two-way fractional bandwidths are measured by pulsing with a 16-period square wave at discrete frequencies using a Tektronix AGF3102C arbitrary function generator. The peak-to-peak output pressures are measured with a hydrophone by pulsing with a 5 MHz, two-period square pulse. The hydrophone and plane reflector measurements are carried out with an AC voltage of ± 10 V and a DC voltage corresponding to 80% of the pull-in voltage.

The table shows the measured pull-in voltages, center frequencies, peak-to-peak output pressures, maximum peak-to-peak pulse-echo signals and -6 dB fractional bandwidths for the fabricated CMUTs. An optimum in both peak-to-peak output pressure and pulse-echo signal is seen for the 9.3 μm plate, which still has a moderate bandwidth of 60%. In fact, the 9.3 μm plate results in a 1.9 times higher peak-to-peak output pressure and a 3.6 times higher pulse-echo signal compared to the 2 μm plate. On the other hand, the highest bandwidth is observed for the 2 μm plate. This study shows that a higher output pressure and pulse-echo signal (evaluated at the center frequency) can be achieved by customizing the plate thickness.

Reference

[1] K. K. Park, H. Lee, M. Kupnik, and B. T. Khuri-Yakub, "Fabrication of Capacitive Micromachined Ultrasonic Transducers via Local Oxidation and Direct Wafer Bonding", *Journal of Microelectromechanical Systems*, vol. 20, no. 1, 2011.

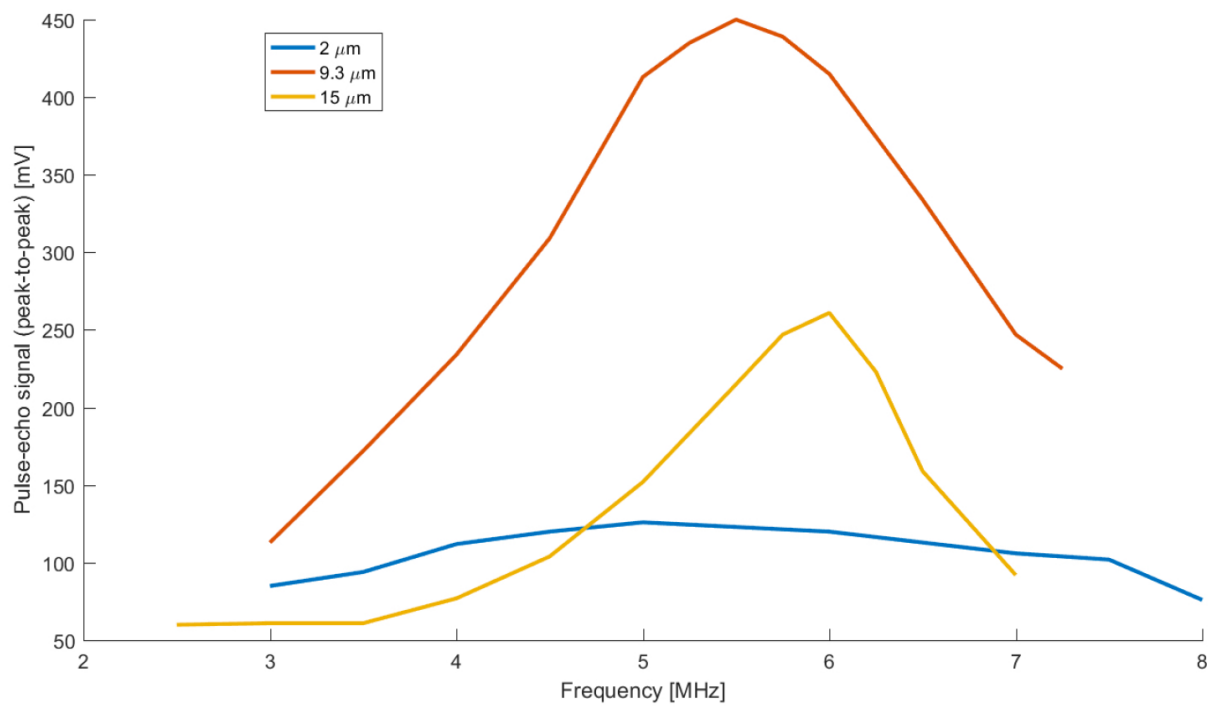


Plate thickness [μm]	Pull-in voltage [V]	Center frequency [MHz]	Peak-to-peak output pressure [kPa]	Peak-to-peak pulse-echo signal [mV]	-6 dB fractional bandwidth in %
2	210	5	203	126	> 100
9.3	200	5.5	380	450	60
15	200	6	238	261	30

Analysis and representation of DHM[®] data for MUT and SAW analysis

Yves Emery, Jérôme Parent, Eduardo Solanas, Etienne Cuche

Lyncée Tec SA, Lausanne, Switzerland, yves.emery@lynceetec.com

Digital Holographic Microscope (DHM[®]) used in conjunction with laser pulsed stroboscopic acquisition provides time-sequences of MUT 3D surface topography along the phase of its excitation signal, with a bandwidth of 200 MHz for state-of-the-art systems. Measurement contains both the initial topography and vibration around it and can be displayed as a 4D animation (Fig. 1). To visualize precisely and to quantify phenomenon under investigation it is important to simplify this representation and to extract efficiently meaningful vibration characteristics. This paper presents solutions adapted to MUT characterization and illustrates their respective advantages

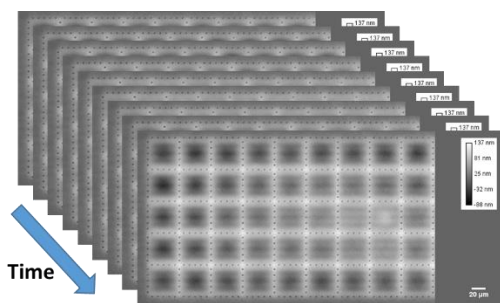


Fig. 1. 3D topographies time-sequence, i.e. 4D topography representation of a MUT array excited at 8 MHz. On a PC display it is naturally represented as a video sequence (Courtesy of IPMS Dresden, Germany)

Vertical displacement of MUT membrane (tens of nanometers) are often small compared to the vertical range of the topography (hundreds of nanometers). This difference of vertical scale prevents visualisation of small vibrations on a 4D representation. Therefore the initial topography is separated from vibrational components by filtering in the frequency domain the height information for each pixel of the field of view. Fig. 2.a shows the vibration time sequence corresponding to Fig. 1. Vibrations are characterized by: vibration amplitude map (Fig. 2.b) and phase vibration map representing the difference between the MUT response and the excitation signal (Fig. 2.c). This data representation enables to identify and analyse efficiently MUT elements behaving differently.

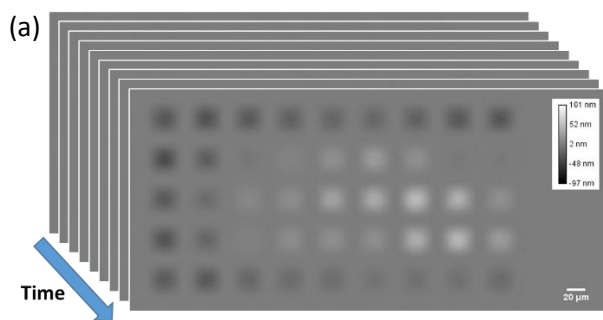
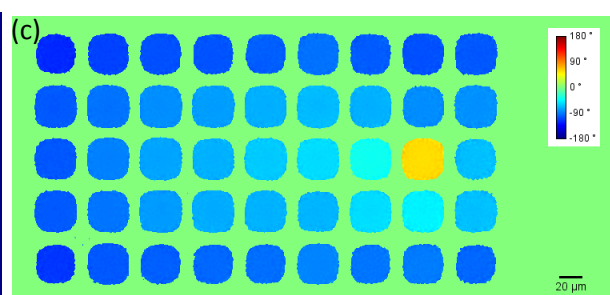
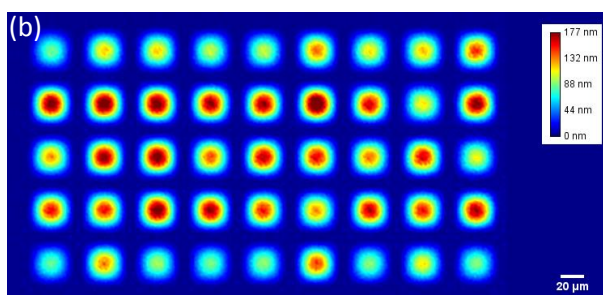


Fig. 2. (a) 4D representation of membrane vibration (AC component), (b) Amplitude vibration map, and (c) Phase vibration map of a MUT device excited at 8 MHz (Courtesy of IPMS Dresden, Germany).



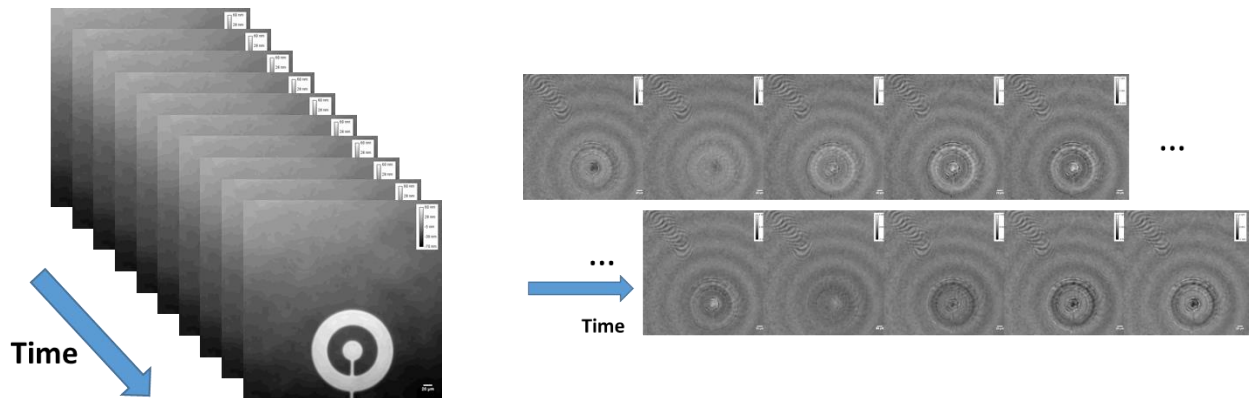


Fig. 3. 4D topography (left) and 4D vibration representation of a MUT excited at 10 MHz and producing SAW. (Courtesy of Q. Wang, D. Horsley, UC Davis, USA)

Fig 3 shows an example of MUT with large vertical structures preventing the visualization of vibrations on the 4D topography representation. Removal of initial topography is necessary to visualize the one nanometer amplitude vibrations. This application shows not only MUT membrane vibrations but also Surface Acoustic Wave (SAW) propagation on the surface of the device. Fig 4 shows that these SAW are non-standing waves. They are evidently not visible as the amplitude has only a small spatial dependence, but are clearly identifiable on the phase map representation. SAW properties can be calculated from this measurement.

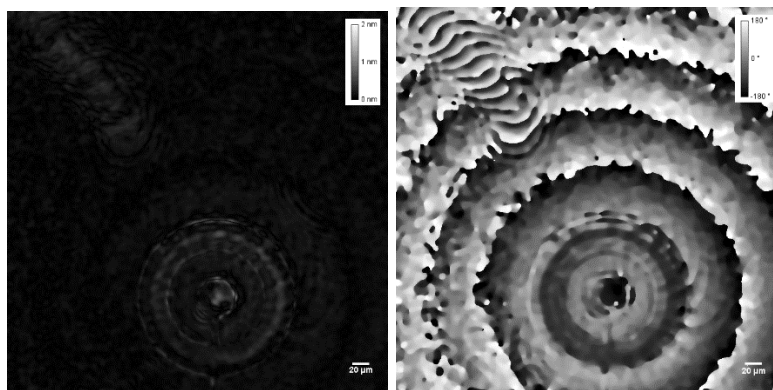


Fig. 4. Amplitude vibration map (left), and Phase vibration map (right) of a MUT device excited at 10 MHz and producing SAW. (Courtesy of Q. Wang, D. Horsley, UC

Amplitude and phase vibration maps are ideal to visualize vibration modes. Uniformity of the MUT devices response and SAW can be efficiently analysed and quantified, and the different behaviour of MUT elements can be identified. Combined with frequency scan, each of them can be then analysed with Bode & Nyquist plots for instance. Profile cuts enable detailed analysis membranes shape and of their dynamical deformation.

DHM[®] used in conjunction with laser pulsed stroboscopic acquisition provides unrivalled wealth of information over the full field of view, without any scanning. Data analysis enables fast visualization, measurement, and understanding of the resonance behaviour of MUT.

